Two types of garnet–clinopyroxene–plagioclase metabasites in the Malá Fatra Mountains crystalline complex, Western Carpathians: Metamorphic evolution, P–T conditions, symplectitic...

Article *in* Petrology · March 2001

Sergey Petrovic. Korikovsky
Russian Academy of Sciences

Petrology, Vol. 9, No. 2, 2001, pp. 119–141. Translated from Petrologiya, Vol. 9, No. 2, 2001, pp. 140–166.

Two Types of Garnet–Clinopyroxene–Plagioclase Metabasites in the Malá Fatra Mountains Crystalline Complex, Western Carpathians: Metamorphic Evolution, *P–T* Conditions, Symplectitic and Kelyphitic Textures

S. P. Korikovsky* and D. Hovorka**

* *Institute of the Geology of Ore Deposits, Petrography, Mineralogy, and Geochemistry, Russian Academy of Sciences, Staromonetnyi per. 35, Moscow, 109017 Russia*
e-mail: korik@igem.ru

** *Faculty of Natural Sciences, Comenius University, Mlynská dolina, Bratislava, 84215 Slovakia*
e-mail: dubikova@fns.uniba.sk

Received August 28, 2000

Abstract—In the pre-Upper Carboniferous Malá Fatra Mts. metamorphic complex in the Western Carpathians, banded amphibolites and amphibole gneisses include *Grt–Cpx–Hbl–Pl* metabasites of two types. Type I comprises massive coarse-grained *Grt–Aug–Hbl–Pl–Qtz* rocks without symplectites and kelyphites. The rocks compose boudins up to a few centimeters across in amphibolites. Their garnet shows prograde zoning with thin outer retrograde rims; the augite (in the matrix and in inclusions in garnet) contains no more than 4% *Jd*; the *An* concentration in the plagioclase is 49–87%; and the brown–green amphibole is classed with low-Na hornblende–tschermakite series. The type-I assemblages suggest a one-stage prograde–retrograde cycle: according to *Grt–Cpx* thermometry, the temperature first increased from 630 to 705°C from the cores to rims of progradely zoned garnet crystals and then decreased to 640°C during the exhumation, when the outermost retrograde rim grew. The type-II metabasites are fine- to medium-grained boudins of *Grt–Cpx–Pl–Qtz* rocks with a *Hbl–Pl–Ilm* ± *Qtz* or *Hbl–Aug* (1–4% *Jd*)–*Pl* (20–40% *An*) ± *Qtz* matrix. In contrast to the type-I metabasites, these rocks contain patches of fine-grained *Aug* (1–4% *Jd*)–*Pl–Hbl–Ttn* symplectites, which were previously thought to be produced by the replacement of early omphacite. It was also hypothesized that the type-II metabasites are recrystallized eclogites. However, it was definitely established that omphacite relics are totally absent from these rocks. The garnet has prograde zoning, sometimes with thin retrograde rims, and contains inclusions of *Hbl*, *Ep*, and *Pl* but never armored relics of high-pressure minerals. According to *Grt–Hbl* thermometry, the temperature increased from 600 to 699°C from the cores to rims. This indicates that the *Aug*-bearing symplectites and the analogous matrix were produced not by the recrystallization of eclogites but by the reaction *Hbl* + *Czo* + *Qtz* $\longrightarrow$ *Cpx* + *Pl* +*Grt* (outer prograde rim) + *Ttn* + H_2O, which marks the transition from the epidote amphibolite to amphibolite facies at T_{max} ~700°C (*Grt–Hbl* thermometry) and *P* ~ 8–9 kbar (*Grt–Hbl–Pl–Qtz* barometry). Chemical reactions resulting in symplectites in the metabasites are examined as functions of the bulk-rock (Ca + Al)/(Mg + Fe) ratios and the X_{Fe} values. The very close compositions of minerals in the metabasites of types I and II, similar zoning of their garnets, and their identical *P–T* metamorphic parameters indicate that both rock types underwent a similar one-stage prograde–retrograde evolution from the epidote amphibolite to high-pressure amphibolite facies and a subsequent retrogression. Some differences between the Ca and Al concentrations in the metabasites of types I and II account for their textural dissimilarities and the morphology of *Cpx* crystals in them. Another type of reaction textures in the type-II metabasites is *Pl–Hbl* kelyphite rims (with inner plagioclase and outer hornblende parts) at contacts between garnet and *Cpx–Hbl–Pl* symplectite. The rims are demonstrated to have developed early during the exhumation stage due to the decomposition of the *Grt–Aug* assemblage by the reaction *Grt* + *Cpx* (in symplectite) + Na_2O + H_2O $\longrightarrow$ *Pl* + *Hbl* + *Qtz* in response to decompression and Na inflow at a temperature close to the metamorphic culmination.

INTRODUCTION

The Malá Fatra Mountains is, geologically, a part of basement nose of the Western Carpathians (Fig. 1) and belongs to the mountain chain in the central zone. The ridge consists of two parts: the Vel'ká Lúka and Kriván massifs. The pre-Upper Carboniferous crystalline complexes of the mountain chain are made up of various types of para- and ortho-metamorphic rocks (Ivanov and Kamenický, 1957; Kamenický and Macek, 1984; Méres and Hovorka, 1989; Hovorka and Méres, 1991; Hovorka *et al.*, 1992a; Janák and Lupták, 1997). The metasediments comprise biotite, garnet, and sillimanite paragneisses. The orthogneisses are of tonalitic composition and have an augen structure. The metabasites are dominated by fine- and coarse-grained amphibolites, banded and migmatized amphibolites and amphibole gneisses, and sporadically occurring massive garnet

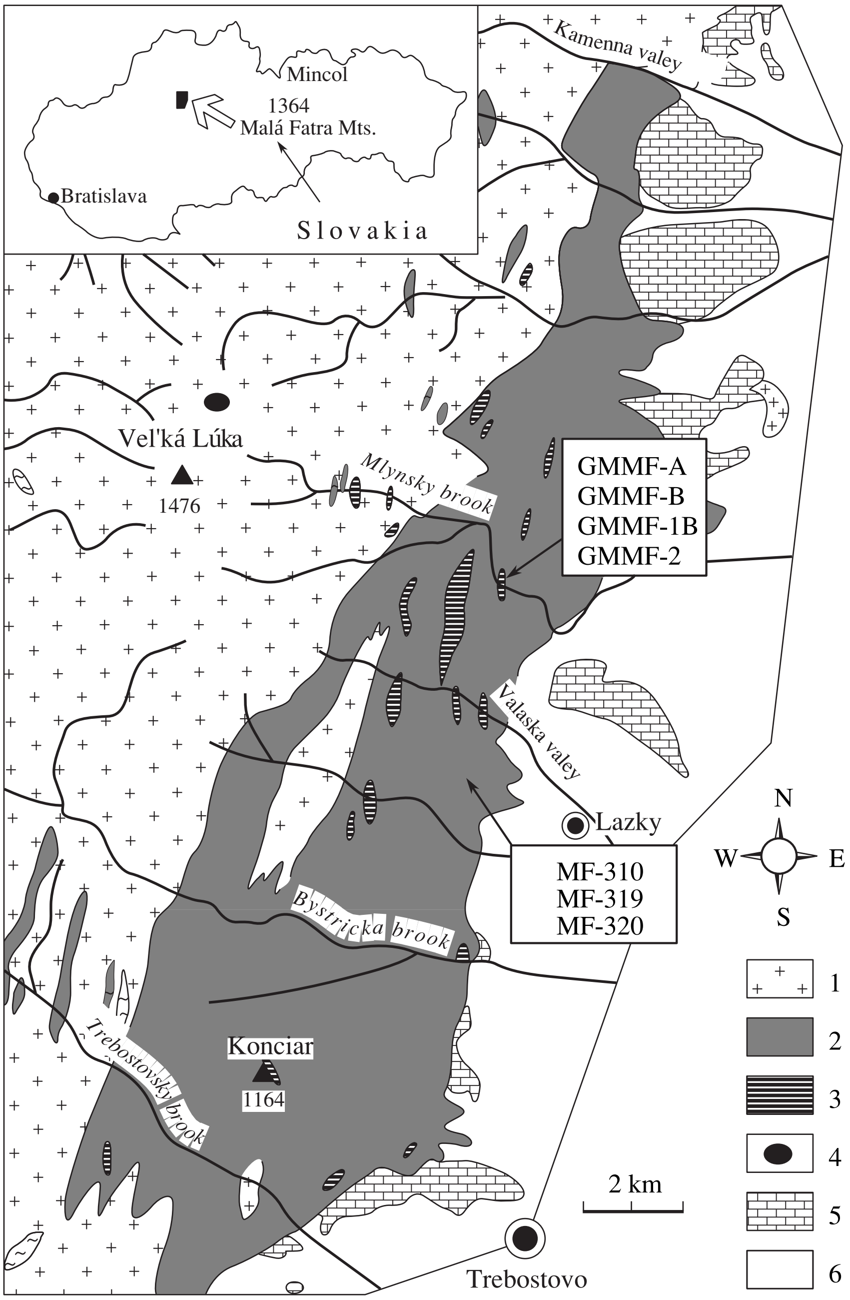

Fig. 1. Schematic geological map of southern Malá Fatra Mts. [modified after (Rakús *et al.*, 1988)].
(1) Hybrid granitoids and tonalites; (2) gneisses and migmatites; (3) amphibolites and migmatized amphibolites; (4) hornblende metaperidotites; (5–6) sedimentary rocks in the cover: (5) Mesozoic, (6) Neogene.

and garnet–clinopyroxene metabasites. The Vel'ká Lúka Massif bears occasional bodies of metaperidotites (Ivanov and Kamenický, 1957; Hovorka *et al.*, 1985; Korikovsky *et al.*, 1998) and calc-silicate rocks (Korikovsky *et al.*, 1987). The bulk of the Malá Fatra Mts. Complex (Fig. 1) is composed of Variscan tonalites, which exhibit intrusive contacts with metamorphic rocks. The U–Pb age of the tonalites is 353 ± 11 Ma (Scherbak *et al.*, 1990).

Our study was centered on the metamorphic conditions of the garnet–clinopyroxene metabasites. These rocks were first described in this complex in the Vel'ká Lúka Massif (Hovorka *et al.*, 1992a; Janák and Lupták, 1997). Similar *Grt–Cpx* metabasites (analogous to type II in this paper) were found and examined in other mountain chains in the Western Carpathians: the Tribec Mountains (Hovorka and Méres, 1990), High Tatry (Hovorka and Méres, 1993; Janák *et al.*, 1996), Nizke Tatry (Hovorka and Méres, 1993; Janák *et al.*, 1995), and Branisko (Hovorka *et al.*, 1997; Méres *et al.*, 2000). They are considered to be a constituent of a leptinite–amphibolite complex, in whose lower part they are contained as relatively small boudins (blocks).

The metamorphic conditions of the Malá Fatra Mts. Complex were extensively discussed elsewhere (Perchuk *et al.*, 1984; Korikovsky *et al.*, 1987; Méres and Hovorka, 1989; Hovorka and Méres, 1991; Hovorka *et al.*, 1992a; Krist *et al.*, 1992; Janák and Lupták, 1997). Some researchers believe that the metamorphism of the crystalline complex was mainly one-stage, prograde, and related to the Variscan cycle, which had its own retrograde stage (Korikovsky *et al.*, 1987). Other geologists considered the complex to be the product of polycyclic metamorphism (Méres and Hovorka, 1989; Hovorka and Méres, 1991; Hovorka *et al.*, 1992, 1997; Janák and Lupták, 1997), with earlier metamorphic events characterized by higher *P–T* parameters, corresponding to the granulite or eclogite facies. The arguments presented in support of a high-pressure stage were derived from the studies of the paragneisses (Méres and Hovorka, 1989; Hovorka and Méres, 1991) and *Grt–Cpx* metabasites (Hovorka *et al.*, 1992a, 1992b; Janák and Lupták, 1997). According to this viewpoint, extensive recrystallization under amphibolite-facies conditions largely obliterated relics of rocks of higher grade, which remain preserved only sporadically or, in places, are totally absent. It is commonly thought that one of the main indications of an early eclogite-facies metamorphic stage and the later recrystallization of the eclogites is *Cpx–Pl* symplectites in some types of the metabasites. However, it is pertinent to mention that real omphacite relics have never been identified in the metabasites of either the Malá Fatra Mts. Complex or the aforementioned complexes in the Western Carpathians. During fieldworks at the Vel'ká Lúka Massif, Hovorka *et al.* (1992a) discovered that the leptinite–amphibolite series includes previously unknown *Grt–Cpx* metabasites with fully equilibrium textures and without secondary reaction symplectites (type I in accordance with the terminology adopted in this paper, see below). These rocks provided valuable information on the nature of the garnet–clinopyroxene rocks.

This paper reports new data on the mineralogy and phase relations of the Malá Fatra Mts. metabasites. These data provided insight into the genesis of these rocks and their reaction textures and, in particular, made it possible to demonstrate that these textures can readily be explained without an early eclogitic metamorphic event.

GEOLOGY OF THE METABASITES

Below, we will briefly characterize the common features of metabasites in the crystalline basement of the Malá Fatra Mts. Complex. Based on their mineralogy, the metabasites are classified into two types (types I and II, see below). Both types occur in the leptinite–amphibolite complex (according to Hovorka and Méres, 1993; Hovorka *et al.*, 1992b, 1994, 1997) or the succession of banded amphibolite rocks (Spišiak and Pitoňák, 1992). In general, the complex is a banded series, whose hornblende amphibolites (sometimes with minor cummingtonite and garnet) alternate with leucocratic plagioclase–quartz–biotite–amphibole–garnet gneisses (leptinites). The complex is extensively migmatized and affected by anatexis. The nature of its protolith is not fully clear. The protolith seems to have been dominated by igneous rocks, which were later metamorphosed mainly to the amphibolite facies (Hovorka *et al.*, 1997).

Metabasites of type I were studied in exposures along a timberland road between the village of Bystrička and Valaská valley, 2 km west of the settlement of Lazky (Fig. 1, Samples MF-310, MF-319, and MF-320). The metabasites are medium- to coarse-grained garnet–clinopyroxene massive rocks with minor plagioclase and hornblende. The "nests" or boudins vary from a few to a few dozen cubic centimeters in volume (Fig. 2a). The boudins are hosted by banded amphibolites and amphibole gneisses with alternating melanocratic and more leucocratic layers, which are composed of hornblende, acid and intermediate plagioclase, and quartz but never garnet. Along the strike, boudins of garnet–clinopyroxene rocks grade into amphibolites, with the lineation of the metabasites conformable with the schistosity of the host amphibolites at the tapering of the boudins. At the same time, the boundaries between *Grt–Cpx* metabasites and amphibolites are sharp in directions perpendicular to their contact, where the massive fabric of metabasites is clearly different from the plane-parallel textures of amphibolites. We examined and analyzed mineral assemblages mainly from the outermost zones of *Grt–Cpx* boudins, which contain, in addition to clinopyroxene and garnet, equilibrium amphibole, plagioclase, and quartz, i.e., associations transitional to the amphibolites. The chemistry of minerals were determined to be identical in the inner and outer portions of the garnet–clinopyroxene bodies.

Metabasites of type II were encountered as lenticular boudins, ranging from a decimeter to a meter across, in Mlynský brook valley west of the town of Turčiansky Martin (Fig. 1, Samples GMMF-A, GMMF-B, GMMF-1B, and GMMF-2. The rocks are fine- and medium-grained and consist of garnet, clinopyroxene, hornblende, and plagioclase. Boudins of this composition were found in the basal portion of the leptinite–amphibolite complex. They are zoned (Hovorka and Méres, 1989; Hovorka *et al.*, 1992a, 1994, 1997; Janák *et al.*, 1997), with cores consisting of the *Grt* + *Cpx* + *Rt* ± *Hbl* assemblage and peripheries containing plagioclase and higher concentrations of hornblende. The main difference of these rocks from the type-I metabasites is symplectitic aggregates of the *Cpx–Pl* or *Hbl–Cpx–Pl* composition, which suggest that the cores of the lenses once contained the *Omp* + *Grt* eclogite

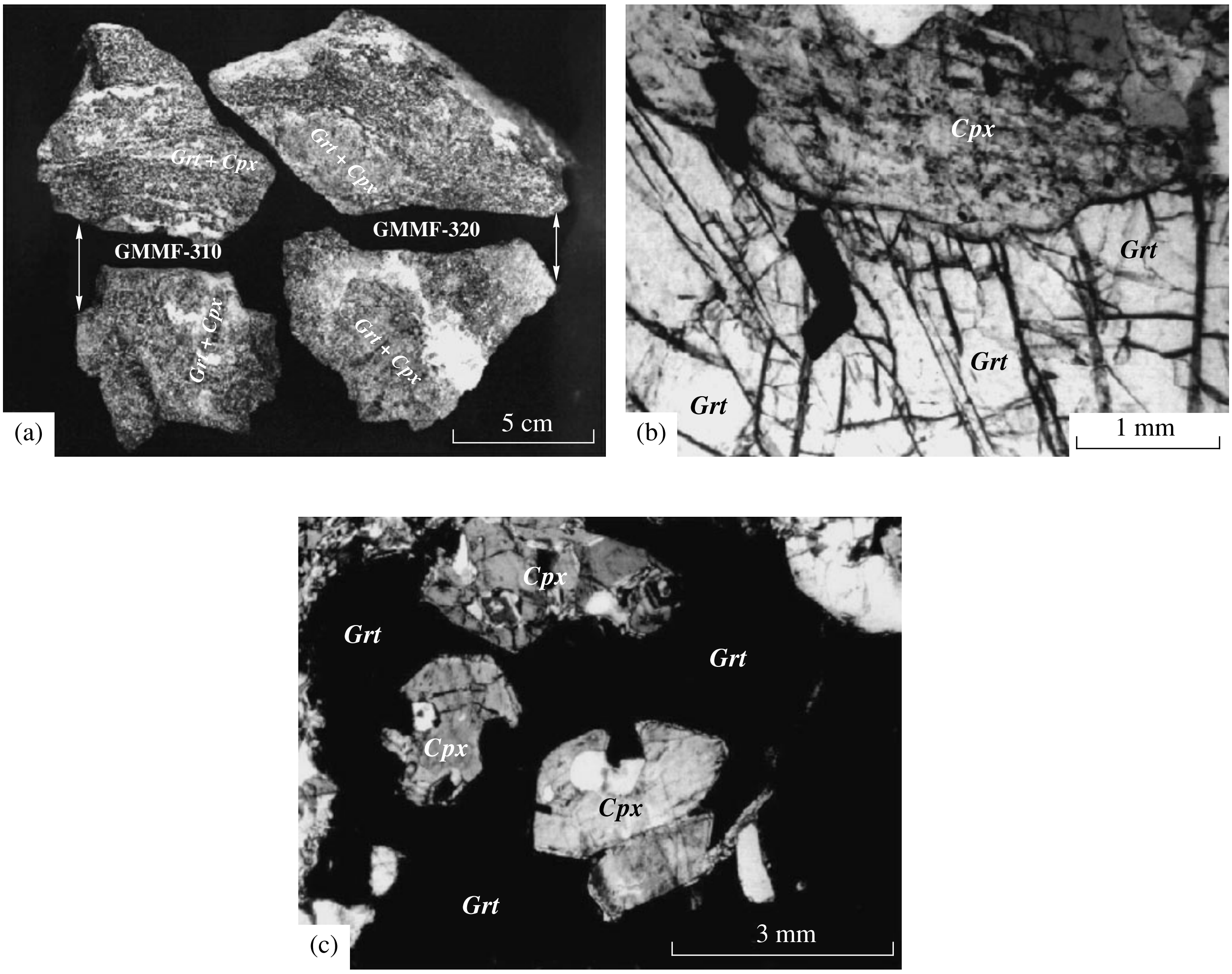

Fig. 2. Metabasites of type I.

(a) Banded plagioclase amphibolite with "nests" and boudins (3–5 cm in diameter) of coarse-grained *Grt–Cpx–Hbl–Pl–Qtz* metabasites (Samples MF-310 and MF-320).

(b–c) Thin-section photomicrographs: (b) contact between garnet and augite crystals in coarse-grained metabasite (Sample MF-310, parallel polarizers), (c) inclusions of augite crystals in garnet. White crystals are quartz (Sample MF-310, crossed polarizers).

assemblage, which was later hydrated under amphibolite-facies conditions. This can be inferred from the fact that the mineral assemblages of the outer zones are identical to the assemblages in the host banded amphibolites. We studied petrographic thin sections and mineral equilibria from the intermediate zones of boudins, which is transitional from their plagioclase-free cores of *Grt–Cpx–Rt* composition to the surrounding garnet-free amphibolites (Fig. 3d).

PETROGRAPHY

The rock-forming minerals of the garnet–clinopyroxene amphibolites of both types (Table 1) are garnet, hornblende, clinopyroxene, plagioclase, and quartz, occasional biotite; the accessories are ilmenite, rutile, and titanite. In accordance with the rock textures, the habit of clinopyroxene crystals, and, particularly, the relationships between the clinopyroxene, garnet, amphibole, and plagioclase, the amphibolites can be subdivided into two groups.

As was defined above, **type I** comprises boudins of coarse-grained garnet–clinopyroxene–plagioclase metabasites (Samples MF-310 and MF-320), which sometimes grade into garnet amphibolites (Sample MF-319, Table 1). In these rocks, round garnet crystals (1–1.5 cm, 10–20 vol %) occur in physical contact (without any reaction textures) with large crystals of augitic clinopyroxene (Fig. 2b) and abound in smaller clinopyroxene inclusions of the same composition (Fig. 2c), brown–green hornblende, and occasional armored clinozoisite relics. Garnet crystals are submerged in a medium-grained matrix of euhedral augite (2–3 mm), brown–green hornblende, calcic plagioclase (50–87% *An*), and quartz, with all minerals occurring in textural equilibrium with one another. The accessories

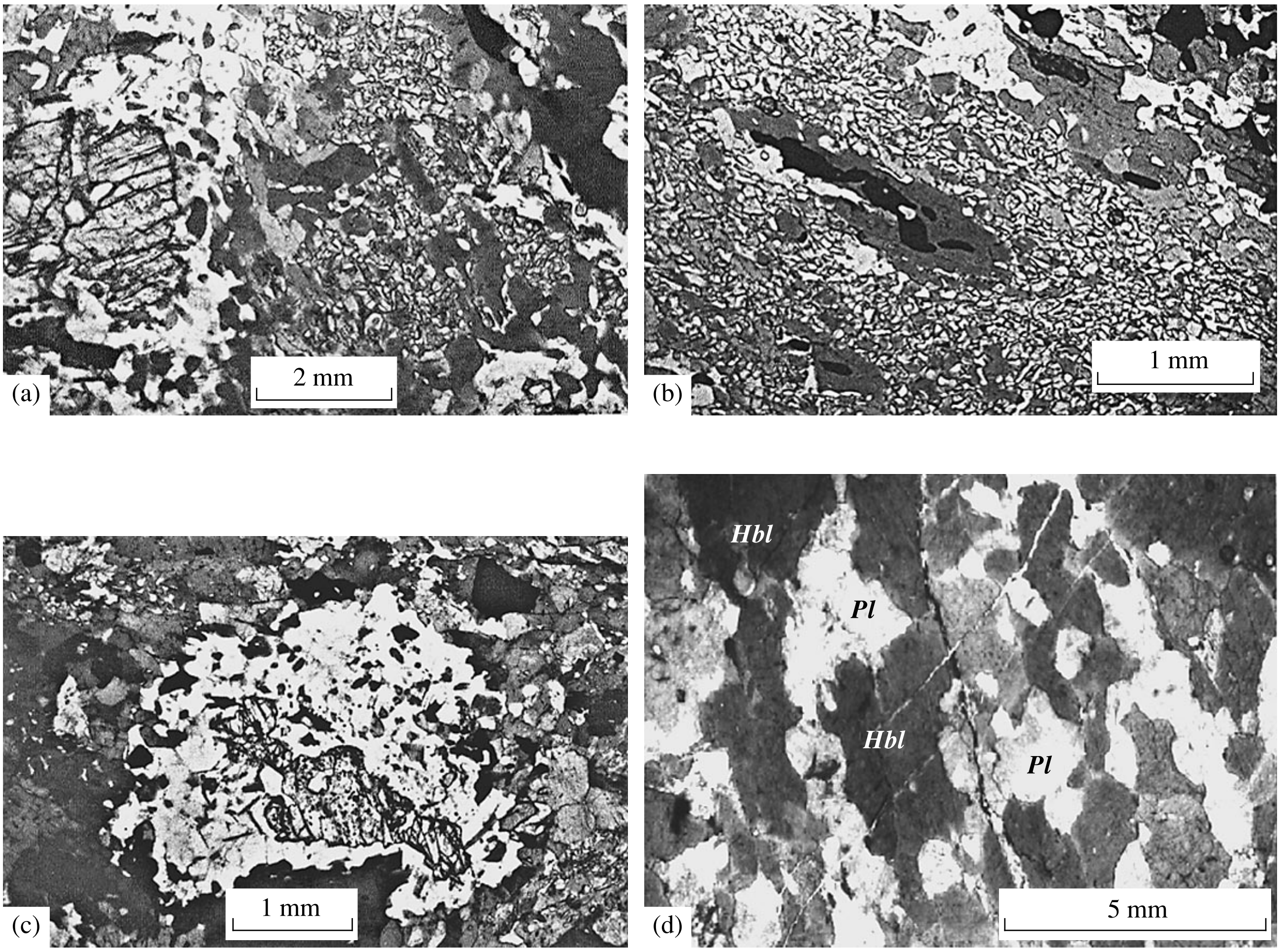

Fig. 3. Metabasites of type II, thin-section photomicrographs.

(a) Photomicrograph of metabasite: garnet crystal contains *Pl* and *Ep* inclusions and is surrounded by a *Pl* (±*Hbl*) inner and a *Hbl* (±*Pl*) outer rim, which separate *Grt* from fine-grained *Cpx*–*Hbl*–*Pl* ± *Ttn* symplectite (matrix) with inclusions of large crystals of primary *Hbl* (dark). The top right part of the photo shows a fragment of a much coarser grained *Hbl*–*Ilm*–*Pl* matrix (Sample GMMF-B, parallel polarizers).

(b) Fine-grained *Cpx*–*Hbl*–*Pl* symplectite with approximately equal proportions of *Cpx* (light gray) and *Hbl* (dark gray) and a slightly resorbed (in the margins) large *Hbl* crystal, which contains *Ilm* inclusions. The top right corner of the photo shows a fragment of the coarse-grained *Hbl*–*Pl*–*Ilm* ± *Ttn* matrix (Sample GMMF-A, parallel polarizers).

(c) Garnet containing *Hbl* and *Czo* inclusions and surrounded by a doubled kelyphite rim in contact with *Cpx*-bearing symplectite or matrix. Inner rim is nearly monomineralic plagioclase (±*Hbl*), outer rim is monomineralic hornblende (±*Pl*). The periphery of the *Hbl* rim contains remnants of *Cpx*–*Hbl*–*Pl* symplectite in the form of small *Pl* fragments, whereas *Cpx* is nearly fully replaced by coarse-grained *Hbl* (Sample GMMF-2, parallel polarizers).

(d) Plagioclase amphibolite with a plane–parallel nematogranoblastic texture from the host banded complex, which contains boudins and "nests" of *Grt*–*Cpx*–*Hbl*–*Pl* metabasites (Sample GMMF-D, parallel polarizers).

are ilmenite and rutile, which are often armored by titanite rims. The type-I metabasites do not contain either omphacite or *Cpx*–*Pl* symplectites. Although no chemical analyses of the rocks were available, the abundance of such high-Ca minerals (Table 1) as labradorite–bytownite, nearly Na-free clinopyroxene, grossular-bearing garnet, low-Na hornblende (Tables 2, 3, 6, and 7), and clinozoisite inclusions in garnet definitely suggests that the metabasites of type I are enriched in Ca, as compared with surrounding *Cpx*-free amphibolites, and resemble most closely metamorphosed enclaves of Ca–Fe–Mg aluminosilicate rocks in the banded leptinite–amphibolite complex.

Secondary alterations are manifested in the type-I metabasites in the form of titanite rims around ilmenite and rutile crystals and in such apparently retrograde textures as thin selvages of pale green amphibole around primary hornblende and augite crystals and the partial replacement of these primary minerals by epidote and chlorite aggregates. The type-I garnet–clinopyroxene rocks bear no kelyphites or symplectites.

The garnet–clinopyroxene metabasites of **type II** (Samples GMMF-2, GMMF-B, GMMF-1B, GMMF-A,

Table 1. Modal composition of garnet- and clinopyroxene-bearing metabasites

Mineral	Primary minerals of the granoblastic matrix								Symplectites in the matrix			
	Grt	*Cpx*	*Hbl*^{1}	*Bt*	*Pl*	*Qtz*	*Ilm*	*Rt*	*Cpx*	*Hbl*	*Pl*	*Ttn*
Type I												
MF-310	+	+	+	–	+	+	+	±		–		
MF-320	+	+	+	–	+	+	+	±		–		
MF-319	+	–	+	+	+	+	+	–		–		
Type II												
GMMF-2	+	+	+	+	+	–	+	–	+	+	+	+
GMMF-B	+	+	+	–	+	–	+	–	+	+	+	+
GMMF-1B	–	–	+	+	+	+	–	–	–	–	–	–
GMMF-A	+	–	+	+	+	–	+	–	+	+	+	±

Mineral	Inclusions in *Grt* crystals						High-T^o rims		Medium-T^o secondary minerals		
	Cpx	*Hbl*^{1}	*Czo*^{1}	*Pl*	*Qtz*	*Ilm*	*Grt* ⟶ doubled *Pl*-*Hbl* rim	*Ilm*(*Rt*) ⟶ *Ttn* rim	*Hbl*^{2}	*Czo*^{2}	*Chl*
Type I											
MF-310	+	+	–	±	+	+	–	+	+	–	–
MF-320	+	+	+	±	–	+	–	+	+	+	+
MF-319	–	+	+	+	+	–	–	–	±	–	–
Type II											
GMMF-2	–	+	+	+	+	+	+	–	±	+	–
GMMF-B	–	+	+	+	+	+	+	–	±	+	–
GMMF-1B	–	+	–	+	+	+	–	–	±	+	+
GMMF-A	–	+	+	+	+	–	+	–	±	–	–

Table 1) are similar mineralogically but have finer grained massive textures. The matrix consists of fine-grained nematogranoblastic hornblende–clinopyroxene–plagioclase or medium-grained hornblende–plagioclase aggregates, which are either quartz-free (Table 1) or contain quartz in insignificant amounts. Ilmenite is sometimes very abundant, up to 5–6%. The usual accessories are apatite and titanite (without inclusions of rutile relics).

The main distinctive feature of the amphibolites of type II is the occurrence in them of independent *Cpx*–*Pl*–*Hbl*–*Ttn* symplectites and doubled *Pl*–*Hbl* kelyphitic rims around garnet (Fig. 3a). The fine-grained symplectitic aggregates have amoeba-shaped contours and range from 1 to 5–8 mm. They are not bimineralic (*Cpx* + *Pl*) but consist of roughly equal proportions of three minerals: augite, brown–green hornblende, and oligoclase with a minute titanite admixture. No omphacite relics were identified within the symplectites of the samples. The aggregates are symplectitic, dactylitic, or granoblastic in texture, they account for 25–30% of the rock volume, and appear as part of the matrix. In addition to small amphibole crystals, which are commensurable with analogous *Cpx* and *Pl* crystals, symplectites often contain large crystals of brown–green hornblende (Fig. 3a), sometimes in aggregates with ilmenite (Fig. 3b), which displays apparent evidence of marginal resorption by *Cpx*–*Pl* aggregates. Fine-grained *Cpx*–*Hbl*–*Pl* ± *Ttn* symplectite alternates with medium- and coarse-grained *Cpx*-free *Hbl*–*Ilm*–*Pl* ± *Qtx* matrix (Figs. 3a, 3b). The amounts of symplectites decrease toward the margins of *Grt*–*Cpx*–*Hbl*–*Ilm*–*Pl* ⟶ *Qtz* boudins, whereas the percentage of the *Hbl*–*Pl* matrix increases, and the rocks grade into normal *Hbl*–*Pl*–*Qtz* amphibolites with a plane-parallel nematogranoblastic texture (Fig. 3d).

Garnet crystals range from 2 to 6 mm in size, have a subhedral habit with slightly resorbed contours, and are surrounded by doubled kelyphitic rims (Figs. 3a, 3c): an inner (closer to garnet and fully enveloping it) nearly monomineralic rim of acid plagioclase (oligoclase or andesine) and minor fine-grained green hornblende and an outer rim (closer the clinopyroxene-bearing matrix or to clinopyroxene-bearing symplectites) of nearly monomineralic hornblende. The brown–green coarse-grained amphibole in the outer rim partly replaces small clinopyroxene crystals in the adjacent symplectite (Fig. 3c), a fact pointing to the later development of

Table 2. Microprobe analyses of a garnet crystal with *Cpx* inclusions and minerals from the adjacent *Hbl–Cpx–Pl* matrix in garnet–clinopyroxene–amphibole–plagioclase–quartz metabasite (type I, Sample MF-310) and its *Grt–Cpx* geothermometry

Component	Adjacent matrix		*Grt* crystal with *Cpx* inclusions											Adjacent matrix;		
	Pl	*Hbl*	rim		intermediate zone				core		intermediate zone		rim	*Cpx*	*Hbl*	*Pl*
			Grt	*Cpx*	*Grt*	*Cpx*	*Grt*	*Cpx*	*Grt*	*Cpx*	*Grt*	*Cpx*	*Grt*			
	1	2	3	4	5	6	7	8	9	10	11	12	13	14	15	16
SiO_2	47.92	45.30	37.48	51.38	37.45	51.45	37.58	52.01	37.54	52.02	37.33	51.77	37.52	52.13	43.87	46.20
TiO_2	–	1.41	0.03	0.22	0.01	0.23	0.06	0.18	0.01	0.11	0.15	0.14	0.12	0.12	1.75	–
Al_2O_3	33.40	10.48	21.59	1.93	21.51	1.47	20.88	1.16	21.23	1.21	21.38	1.39	21.21	1.23	12.22	34.47
FeO	0.25	17.73	27.98	11.85	28.39	11.94	28.86	11.78	28.81	12.50	28.52	11.96	28.48	11.64	17.29	0.18
MnO	–	0.21	1.14	0.20	1.38	0.20	1.39	0.14	1.49	0.22	1.16	0.21	1.47	0.15	0.14	–
MgO	–	9.77	4.39	11.78	3.77	11.84	3.53	12.00	3.00	11.41	3.86	11.90	3.44	11.75	9.38	–
CaO	16.08	11.96	7.36	22.15	7.46	22.44	7.58	22.46	7.83	22.37	7.54	22.31	7.68	22.65	11.45	17.63
Na_2O	2.13	0.63	–	0.44	–	0.36	–	0.21	–	0.09	–	0.27	–	0.29	1.17	1.47
K_2O	0.04	0.71	–	0.01	–	0.04	–	0.03	–	0.02	–	0.02	–	–	1.07	0.01
Total	99.82	98.20	99.91	99.96	99.97	99.97	99.88	99.97	99.91	99.95	99.94	99.97	99.92	99.96	98.34	99.96
Si	2.19	6.67	2.96	1.95	2.97	1.95	2.99	1.97	2.98	1.97	2.96	1.96	2.98	1.97	6.47	2.13
Al(IV)	1.80	1.33	2.01	0.05	2.01	0.05	1.96	0.03	1.99	0.03	2.00	0.04	1.98	0.03	1.53	1.87
Al(VI)		0.49		0.04		0.02		0.02		0.02		0.02		0.03	0.59	
Ti	–	0.16	–	0.01	–	0.01	–	0.01	–	–	0.01	–	0.01	–	0.19	–
Fe^{3+}	–	0.20		–		–		–		–		–		–	0.18	–
Fe^{2+}	0.09	1.98	1.85	0.38	1.88	0.38	1.92	0.37	1.92	0.40	1.89	0.38	1.89	0.37	1.95	0.01
Mn	–	0.03	0.08	0.01	0.09	0.01	0.09	–	0.10	0.01	0.08	0.01	0.10	–	0.02	–
Mg	–	2.14	0.52	0.66	0.45	0.67	0.42	0.68	0.36	0.64	0.46	0.67	0.41	0.66	2.06	–
Ca	0.79	1.89	0.62	0.90	0.63	0.91	0.65	0.91	0.67	0.91	0.64	0.91	0.65	0.92	1.81	0.87
Na	0.19	0.18	–	0.03	–	0.03	–	0.01	–	0.01	–	0.02	–	0.02	0.33	0.13
K	–	0.13	–	–	–	–	–	–	–	–	–	–	–	–	0.20	–
Alm			60.4		61.6		62.4		63.0		61.7		61.9	–		
Sps			2.5		3.0		3.0		3.3		2.5		3.3			
Prp			16.9		14.6		13.6		11.7		14.9		13.4			
Grs			20.3		20.8		21.0		22.0		22.9		21.4			
Jd, %				3.2		2.8		1.7		0.8		2.0		2.1		
An, %	80.4															86.8
X_{Fe}		0.51	0.78	0.36	0.81	0.36	0.82	0.36	0.84	0.39	0.81	0.36	0.82	0.36	0.51	
T, °C(*Grt–Cpx*)																
(Powell, 1985)			705		665		640		635		670		645			
(Ai, 1994)			635		595		570		570		600		575			

Table 3. Microprobe analyses of a garnet crystal *Grt* with *Cpx* and *Hbl* inclusions and minerals from the adjacent *Hbl–Cpx–Pl* matrix in garnet–clinopyroxene–amphibole–plagioclase–quartz metabasite (type I, Sample MF-320) and its *Grt–Cpx* geothermometry

Component	Adjacent matrix		*Grt* crystal with *Cpx* and *Hbl* inclusions										
	Pl	*Hbl*	rim	intermediate zone				core		intermediate zone		rim	
			Grt	*Grt*	*Cpx*	*Hbl*	*Grt*	*Grt*	*Hbl*	*Grt*	*Hbl*	*Grt*	*Hbl*
	17	18	19	20	21	22	23	24	25	26	27	28	29
SiO_2	56.06	44.46	36.96	37.08	52.48	44.87	37.21	37.19	43.70	37.30	43.70	37.54	51.70
TiO_2	–	1.34	–	0.11	0.21	1.59	–	0.07	1.94	0.11	1.67	0.08	0.15
Al_2O_3	28.08	10.67	21.09	21.65	1.29	11.31	21.18	21.36	12.29	20.97	12.56	21.32	1.85
FeO	0.16	18.25	28.88	28.10	11.27	16.15	28.61	28.87	16.17	28.66	15.40	28.45	12.08
MnO	–	0.25	2.09	1.43	0.06	–	1.55	1.54	–	1.19	–	1.81	0.18
MgO	–	9.29	2.83	4.02	12.05	10.92	4.14	3.72	10.52	4.38	10.79	3.28	11.55
CaO	10.08	11.66	7.98	7.51	22.37	11.42	7.29	6.86	10.91	7.08	11.14	7.49	22.22
Na_2O	5.49	1.10	–	–	0.23	1.55	–	–	1.83	–	1.79	–	0.22
K_2O	0.02	0.81	–	–	–	0.57	–	–	0.88	–	1.15	–	0.02
Total	99.89	97.83	99.83	99.90	99.96	98.38	99.98	99.60	98.24	99.69	98.20	99.97	99.97
Si	2.52	6.62			1.98	6.54			6.40		6.41		1.96
Al(IV)	1.49	1.38			0.02	1.46			1.60		1.59		0.04
Al(VI)		0.49			0.04	0.48			0.52		0.58		0.05
Ti	–	0.15			0.01	0.17			0.21		0.18		–
Fe^{3+}		0.18			–	0.24			0.26		0.20		–
Fe^{2+}	0.01	2.08			0.36	1.73			1.71		1.69		0.38
Mn	–	0.03			–	–			–		–		0.01
Mg	–	2.06			0.68	2.37			2.29		2.36		0.65
Ca	0.49	1.87			0.90	1.78			1.71		1.75		0.90
Na	0.48	0.32			0.02	0.44			0.52		0.51		0.02
K	–	0.15			–	0.11			0.16		0.21		–
Alm			62.4	60.7			61.0	63.3		61.3		62.2	
Sps			4.6	3.1			3.3	3.4		2.6		4.0	
Prp			10.9	15.4			15.7	14.6		16.7		12.8	
Grs			22.1	20.8			20.0	19.2		19.4		21.0	
Jd, %					1.7								1.7
An, %	50.3												
X_{Fe}		0.53	0.85	0.80	0.34	0.45	0.80	0.81	0.46	0.78	0.44	0.83	0.37
T, °C(*Grt–Cpx*)													
(Powell, 1985)				665								640	
(Ai, 1994)				595								575	

the *Pl–Hbl* rims than the crystallization of the symplectites. As a result, garnet in the type-II metabasites is blocked by doubled *Pl–Hbl* rims and never occurs in physical contact with clinopyroxene, in contrast to the situation in the type-I metabasites.

Another difference from the type-I rocks is that these rocks never contain clinopyroxene inclusions in garnets. The only inclusions are hornblende, plagioclase, clinozoisite, ilmenite, quartz. Judging from the deficit of quartz in the type-II metabasites, their high concentrations of Ti-bearing minerals (ilmenite and titanite), the protolith of these rocks most probably consisted of magmatic mafic rocks with elevated Ca concentrations, which were, however, lower than those in

Table 4. Microprobe analyses of garnet crystals *Grt* with *Ep* and *Hbl* inclusions and minerals from the adjacent *Pl* ± *Hbl* matrix in garnet–clinopyroxene–amphibole–plagioclase–quartz metabasite (type II, Sample GMMF-2) and its *Grt*–*Hbl* and *Grt*–*Hbl*–*Pl*–*Qtz* geothermobarometry

Component	Crystal 1								Crystal 2									
	Grt with *Ep* and *Hbl* inclusions						adjacent *Pl* ± *Hbl* rim		*Grt* with *Ep* and *Hbl* inclusions								adjacent *Pl* ± *Hbl* rim	
	core		intermediate zone			rim			core	intermediate zone					rim			
	Ep	*Grt*	*Grt*	*Grt*	*Grt*	*Grt*	*Hbl*	*Pl*	*Grt*	*Grt*	*Grt*	*Hbl*	*Grt*	*Grt*	*Ep*	*Grt*	*Hbl*	*Pl*
	30	31	32	33	34	35	36	37	38	39	40	41	42	43	44	45	46	47
SiO_2	38.39	37.67	37.61	37.15	37.57	37.82	41.99	56.39	36.97	37.27	37.31	44.27	37.56	37.28	38.53	37.50	42.79	56.96
TiO_2	0.11	0.11	0.02	0.23	0.11	0.08	0.97	–	0.07	0.12	0.09	1.06	0.02	0.06	0.09	0.09	1.51	–
Al_2O_3	28.88	21.53	21.46	21.30	21.44	21.63	14.28	27.31	21.19	21.13	21.29	12.26	21.61	21.44	30.40	21.35	12.64	27.13
FeO*	6.94*	26.66	26.57	27.25	26.62	26.83	18.12	0.52	29.74	29.16	28.53	17.47	27.48	28.24	4.66*	27.45	17.81	0.28
MnO	0.12	1.05	0.92	1.03	0.89	1.03	0.16	–	1.23	1.47	1.64	0.09	1.59	1.53	0.14	1.79	0.30	–
MgO	–	2.34	2.56	2.78	2.84	3.15	8.33	0.03	2.26	2.20	2.20	9.43	2.64	2.75	–	2.88	8.75	–
CaO	23.33	10.56	10.68	10.05	10.45	9.43	11.24	9.09	8.36	8.50	8.90	11.33	9.03	8.61	23.68	8.83	11.32	8.23
Na_2O	0.02	–	–	–	–	–	1.85	6.49	–	–	–	1.61	–	–	0.04	–	1.58	6.84
K_2O	0.05	–	–	–	–	–	0.99	0.06	–	–	–	0.63	–	–	–	–	0.92	0.48
Total	97.84	99.92	99.82	99.79	99.92	99.97	97.93	99.89	99.82	99.85	99.96	98.14	99.93	99.91	97.54	99.89	97.62	99.64
Si	6.06	2.98	2.98	2.95	2.97	2.98	6.26	2.54	2.96	2.98	2.98	6.52	2.98	2.97	6.02	2.98	6.40	2.56
Al(IV)		2.01	2.00	2.00	2.00	2.01	1.74	1.45	2.00	1.99	2.00	1.48	2.02	2.01		2.00	1.60	1.44
Al(VI)	5.36						0.77					0.65			5.60		0.63	
Ti	0.01	0.01	–	0.01	0.01	–	0.11	–	–	0.01	0.01	0.12	–	–	0.01	0.01	0.17	–
Fe^{3+}	0.82						0.21					0.20			0.55		0.18	
Fe^{2+}	–	1.76	1.76	1.81	1.76	1.77	2.05	0.02	1.99	1.95	1.90	1.95	1.82	1.88	–	1.82	2.05	0.01
Mn	0.02	0.07	0.06	0.07	0.06	0.07	0.02	–	0.08	0.10	0.11	0.01	0.11	0.10	0.02	0.12	0.04	–
Mg	–	0.28	0.30	0.33	0.33	0.37	1.85	–	0.27	0.26	0.26	2.07	0.31	0.33	–	0.34	1.95	–
Ca	3.95	0.89	0.91	0.86	0.89	0.80	1.79	0.44	0.72	0.73	0.76	1.79	0.77	0.74	3.96	0.75	1.81	0.40
Na	0.01	–	–	–	–	–	0.53	0.57	–	–	–	0.46	–	–	0.01	–	0.46	0.60
K	0.01	–	–	–	–	–	–	–	–	–	–	0.12	–	–	–	–	0.18	0.03
Alm		58.7	58.1	59.1	57.9	58.9			65.0	64.1	62.7		60.6	61.7		60.0		
Sps		2.3	2.0	2.2	2.0	2.3			2.7	3.3	3.7		3.6	3.4		4.0		
Prp		9.2	10.0	10.8	11.0	12.3			8.8	8.7	8.6		10.4	10.7		11.3		
Grs		29.8	29.9	27.9	29.1	26.5			23.5	23.9	25.0		25.4	24.2		24.8		
An, %								43.5										38.9
X_{Fe}		0.87	0.85	0.85	0.84	0.83	0.55		0.88	0.88	0.88	0.51	0.85	0.85		0.84	0.54	
T, °C(*Grt*–*Hbl*) (Powell, 1985)						699					601					648		
P_s (*Grt*–*Hbl*–*Pl*–*Qtz*) (Kohn and Spear, 1990)						8.8										8.2		

*All iron as FeO.

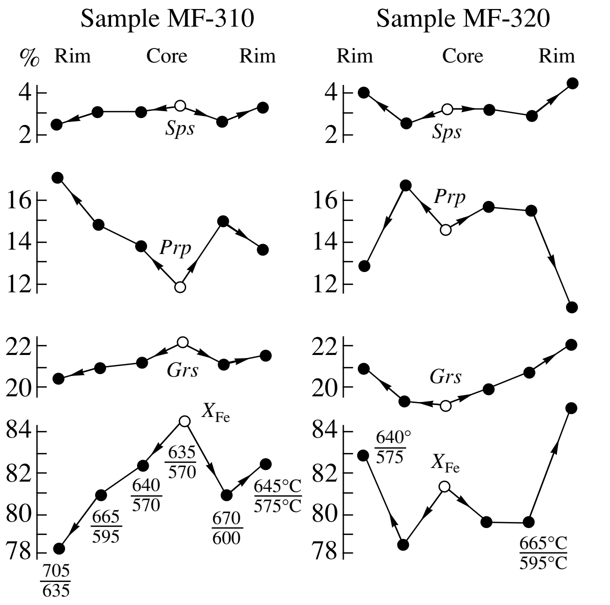

Fig. 4. Microprobe profiles across garnet crystals with *Cpx* and *Hbl* inclusions in coarse-grained *Grt–Cpx–Hbl–Pl–Qtz* metabasites of group I.

Numerator is *Grt–Cpx* thermometry after Powell (1985), denominator is *Grt–Cpx* thermometry after Ai (1994).

the rocks of type I. The nearly plagioclase- and quartz-free cores of boudins in the type-II metabasites may have been metamorphosed melanocratic cumulates in the primary basites.

The retrograde alterations of the rocks are the same as in rocks of type I.

Hence, the main paragenetic differences between metabasites of the two types are as follows:

(1) Type-I metabasites are coarser grained, display equilibrium relationships of their *Aug*, *Grt*, *Hbl*, and high-Ca plagioclase, bear no symplectites, and contain augite both in the matrix and in inclusions in progradely zoned garnet crystals.

(2) Type-II metabasites are finer grained, contain *Aug–Hbl–Olg* ± *Ttn* symplectites, augite occurs in them only in the matrix and in symplectites in association with oligoclase–andesine (but not with labradorite–bytownite, as in type I) and is absent among inclusions in garnet. The garnet was, perhaps, in equilibrium with the matrix or symplectitic augite-bearing aggregates, but later this equilibrium was disrupted and, as a result, the garnet is separated from augite by doubled *Pl–Hbl* kelyphites. These facts point to the somewhat different protolith chemistry and petrological evolution of metabasites of the two groups.

MINERAL CHEMISTRY

All of the microprobe analyses were carried out on a CamScan 4DV microprobe equipped with a Link AN 10000 analytical system at the Geological Department of the Moscow State University at 15 kV accelerating voltage and 1.2×10^{-9} Å beam current.

Garnet

We ran full microprobe profiles across two garnet crystals in type-I metabasites, and analyzed clinopyroxene and hornblende inclusions in these crystals. The garnet was determined to be zonal. In Sample MF-310 (Table 2, Fig. 4), the garnet shows prograde zoning from the core to rim. In one portion (Fig. 4, left), the zoning extends up to the very margin of the grain, whereas in the other part (Fig. 4, right), it gives way to retrograde zoning in the outer margin. In the prograde portions of the crystals, the *Prp* concentration increases from 12 to 17% from the core to margin at a constant *Grs* concentration and a minor *Sps* admixture. In the retrograde outer margin (Fig. 4, right), the *Prp* concentration decreases, and the X_{Fe} changes correspondingly.

In the garnet from Sample MF-320 (Table 3, Fig. 4), prograde zoning is preserved solely in the core (at an increase in the pyrope content, decrease in X_{Fe}, and a roughly constant *Grs* content). In the margins, prograde zoning gives way to retrograde profiles.

In the garnet–clinopyroxene metabasites of type II, the zoning of garnet is similar. In Sample GMMF-2, in spite of the fact that the garnet is surrounded by *Pl–Hbl* rims, the zoning of two crystals (Table 4, Fig. 5) is apparently prograde in terms of *Prp* concentration and X_{Fe} at slightly increasing concentrations of *Sps* and *Grs*. However, in Sample GMMF-B (Table 5, Fig. 5), the garnet has very weak prograde zoning (in terms of *Prp* and *Sps* concentrations and X_{Fe}) in the core and displays retrograde alterations in the margins at a reversed trend of the Grs concentration.

In general, the garnets of types-I and -II metabasites have very similar or nearly identical compositions: all of them are highly ferrous (X_{Fe} = 0.78–0.88), preserve prograde zoning in the inner parts of their profiles or even throughout them, are low in pyrope (8–17%) and very low in spessartine (2–4%). However, the grossular concentration is higher in garnet from the metabasites of type II (23–30%) than in those of type I (19–23%).

Clinopyroxene

The clinopyroxene in the rocks of both groups has a very uniform composition, regardless of the grain morphology and mineral assemblages. The pyroxenes of the type-I metabasites (in the coarse-grained matrix and inclusions in garnet (Tables 1, 2, 6), and the pyroxenes of the type-II metabasites (in the fine-grained matrix and *Cpx–Hbl–Pl–Ttn* symplectites) belong to nearly pure augite (diopside–hedenbergite; Fig. 6) with very insignificant admixtures of jadeite (1–4.5%) and acmite (0–2%) and with X_{Fe} = 0.34–0.39. All clinopyroxene crystals are homogeneous. No relics of more sodic clinopyroxene (with *Jd* > 5%) were detected.

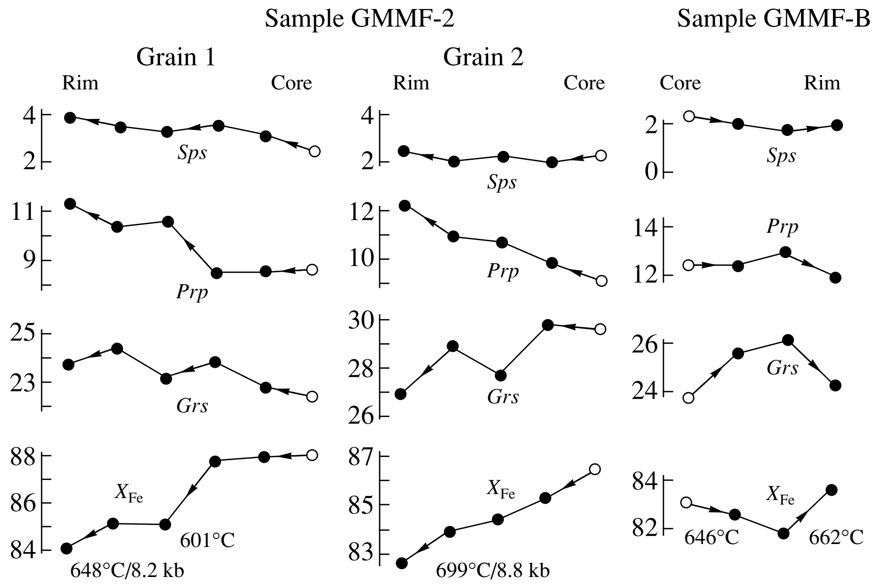

Fig. 5. Microprobe profiles across garnet crystals that contain *Hbl* and *Ep* inclusions and are surrounded by *Pl–Hbl* rims in *Grt–Cpx–Hbl–Pl–Qtz* metabasites of type II.
Grt–Hbl thermometry is after Powell (1995), *Grt–Hbl–Pl–Qtz* barometry is after Kohn and Spear (1990).

Hornblende

All primary brown–green and green hornblendes in the clinopyroxene–garnet rocks of the two groups affiliate with the low-Na hornblende–tschermakite series (Leake *et al.*, 1997) with $(Na + K)_A < 0.5$, and nearly identical $Mg/(Mg + Fe^{2+})$ of about 0.5 (Tables 2–5, 7, and Fig. 7) and moderate Ti (1.3–2.0 wt % TiO_2). The data points of amphiboles from the matrix and inclusions in garnet in type-I metabasites and from the type-II rocks (in the matrix, clinopyroxene–amphibole–plagioclase symplectites, doubled *Hbl–Pl* rims around garnet, and in inclusions in garnet) cluster around the hornblende–tschermakite boundary in the classification plot (Fig. 7).

However, the medium-temperature secondary pale green hornblende from reaction rims around clinopyroxene and around primary hornblende is significantly higher in Si (i.e., in the actinolite end-member) and lower in Ti (0.8–0.9% TiO_2), but does not extend beyond the limits of the hornblende group (Leake *et al.*, 1997) (Table 7, Fig. 7).

Amphibole analogous to that described above was previously distinguished as populations *Hbl* III and *Hbl* IV in these rocks (Hovorka *et al.*, 1994, 1997; Janák and Lupták, 1997; Janák *et al.*, 1997). The earliest population, *Hbl* I, reportedly comprised euhedral crystals of Al-pargasite (ferropargasite) in inclusions in garnet cores. The population *Hbl* II (pargasite) was thought to consist of acicular bluish green amphibole in kelyphites around garnet, at physical contacts between the two minerals. We found no pargasitic Ca-amphiboles, but their absence does change anything in the general estimate of the metamorphic parameters.

Plagioclase

The matrix plagioclase of the type-I clinopyroxene–garnet metabasites (Tables 2, 3, 7) is Ca-rich and corresponds to labradorite–bytownite with 49–87% *An*. The group-II amphibolites (Tables 4, 7) contain more acid plagioclase in the matrix, symplectites, and reaction rims around garnet, i.e., the plagioclase is oligoclase–andesine (20–43% *An*). The composition of the plagioclase varies from domain to domain in each sample.

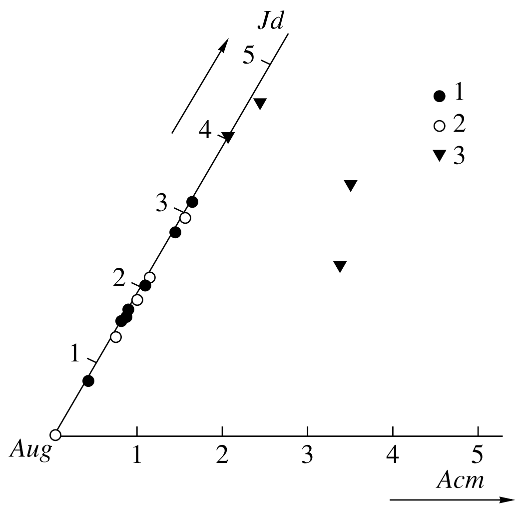

Fig. 6. Composition of clinopyroxene from *Grt–Cpx–Hbl–Pl* ± *Qtz* metabasites plotted in an *Aug–Jd–Acm* diagram.
(1–2) Type-I rocks: (1) large crystals from the matrix, (2) inclusions in *Grt*; type-II rocks: small crystals from *Cpx–Pl–Hbl–Ttn* symplectites and matrix.

Table 5. Microprobe analyses of a garnet crystal with *Hbl* inclusions from garnet–clinopyroxene–amphibole–plagioclase metabasite with *Pl* ± *Hbl* rims around *Grt* (type II, Sample GMMF-B) and its *Grt–Hbl* geothermometry

Component	*Hbl*	*Grt*	*Grt*	*Grt*	*Grt*	*Hbl*
	core		intermediate zone		rim	
	48	49	50	51	52	53
SiO_2	42.38	37.02	37.60	37.35	37.57	42.25
TiO_2	1.81	0.20	0.14	0.09	–	2.04
Al_2O_3	12.92	21.27	21.37	21.21	21.42	12.95
FeO	18.00	28.51	27.32	27.33	28.32	18.69
MnO	–	1.02	0.96	0.81	0.84	0.17
MgO	8.99	3.26	3.22	3.41	3.08	8.48
CaO	11.22	8.63	9.19	9.48	8.70	10.86
Na_2O	1.98	–	–	–	–	1.98
K_2O	1.12	–	–	–	–	0.82
Total	98.42	99.91	99.80	99.68	99.93	98.24
Si	6.30	2.95	2.97	2.96	2.98	6.28
Al(IV)	1.70	1.99	1.99	1.98	2.00	1.72
Al(VI)	0.56					0.55
Ti	0.20	0.01	0.01	0.01	–	0.23
Fe^{3+}	0.16					0.25
Fe^{2+}	2.07	1.90	1.81	1.81	1.88	2.07
Mn	–	0.07	0.06	0.05	0.06	0.02
Mg	1.99	0.39	0.38	0.40	0.36	1.88
Ca	1.79	0.73	0.78	0.81	0.74	1.73
Na	0.57	–	–	–	–	0.57
K	0.21	–	–	–	–	0.16
Alm		61.4	59.7	58.9	61.8	
Sps		2.3	2.1	1.8	1.9	
Prp		12.5	12.5	13.1	12.0	
Grs		23.8	25.7	26.2	24.3	
X_{Fe}	0.53	0.83	0.83	0.82	0.84	0.55
T, °C(*Grt–Hbl*) (Powell, 1985)	646				662	

Plagioclase crystals are homogeneous and display no zoning.

Clinozoisite

Clinozoisite was encountered only in the form of small inclusions in the cores of progradely zoned garnet crystals from the metabasites of types I and II, but is absent in the matrix. This means that the mineral occurs as armored relics of an earlier and lower temperature epidote-amphibolite metamorphic stage. The mineral contains 4.7–6.9% iron (Table 4). In contrast to relict clinozoisite, aggregates of secondary epidote and chlorite replace brown–green hornblende in the margins.

P–T METAMORPHIC PARAMETERS

The study of clinopyroxene and hornblende inclusions in garnet crystals with the prograde or prograde–retrograde zoning, and analyses of garnet margins and matrix minerals in contact with them, allowed us to assay the metamorphic temperature of equilibrium assemblages in the type-I and -II garnet–clinopyroxene rocks by the *Grt–Cpx* and *Grt–Hbl* thermometers (Powell, 1985; Ai, 1994), and pressure by the *Grt–Hbl–Pl–Qtz* barometer (Kohn and Spear, 1990). Bearing in mind that the primary brown–green amphibole of the type-I metabasites is often replaced by secondary blue–green hornblende in the margins, and it is sometimes hard to distinguish the boundaries between distinct amphibole generations, whereas neighboring garnet and clinopyroxene crystals are never separated by secondary minerals (Fig. 2b), we used only the *Grt–Cpx* thermometers for these rocks. We refrained from employing the *Grt–Cpx–Pl–Qtz* barometer (Eckert *et al.*, 1991) for evaluating the pressure, because the results are not fully satisfactory for assemblages with Ca-rich plagioclase. For instance, the pressure assayed by this barometer for the *Grt* + *Cpx* + *Pl* (86.8% *An*) + *Qtz* assemblage (Sample MF-310, Table 2) is 5.3–5.5 kbar, which is an apparent underestimation.

The *P–T* parameters of type-II rocks were assayed only by *Grt–Hbl* thermometers, because *Grt* and *Cpx* never occur in these rocks in physical contacts but are separated by secondary minerals (see above). The pressure was determined by the *Grt–Hbl–Pl–Qtz* barometer, which yields correct estimates for assemblages with plagioclase containing less than 75% *An* (Kohn and Spear, 1990) and hornblende with Na ≤ 0.6 f.u.

The results are compiled in Tables 2–4 and are graphically presented in Figs. 2 and 3.

Metabasites of Type I

Temperature estimates made on the basis of a garnet crystal from Sample MF-310, which has prograde zoning (Fig. 4), demonstrate that the prograde metamorphic temperature increased from 635 to 705°C from the core rimward (metamorphic culmination), according to Powell (1985), or from 570 to 635°C, according to Ai (1994). It is pertinent to mention that the values obtained by Powell's thermometer seem to be more realistic, considering the fact that the metamorphic conditions apparently corresponded to the upper amphibolite facies, in which epidote becomes unstable in the matrix of a rock. In another part of the same garnet grain, which includes a retrograde outer rim, the estimated temperature is as low as 645°C (Powell, 1985), which marks the cessation of exchange reactions

Table 6. Microprobe analyses of clinopyroxene from the matrix and symplectite of garnet–clinopyroxene–amphibole–plagioclase metabasites of types I and II

Component	Type I				Type II			
	Large crystals (often in contact with *Grt*)				Small crystals from *Cpx–Hbl–Pl–Ttn* symplectite (never in contact with *Grt*)			
	MF-310		MF-320		GMMF-2		GMMF-B	
	54	55	56	57	58	59	60	61
SiO_2	51.70	51.46	52.02	52.43	52.36	52.59	52.56	52.13
TiO_2	0.19	0.15	0.06	0.12	0.13	0.19	0.10	0.14
Al_2O_3	1.33	1.77	0.91	1.54	0.99	1.03	0.52	0.77
FeO	11.77	12.57	12.47	12.08	10.91	10.56	11.91	11.82
MnO	0.22	0.09	0.12	–	0.09	0.19	0.29	0.26
MgO	11.71	11.18	10.89	11.60	12.01	12.33	11.71	11.89
CaO	22.78	22.34	23.30	21.91	22.91	22.40	22.22	22.21
Na_2O	0.26	0.41	0.16	0.29	0.56	0.62	0.57	0.67
K_2O	–	–	0.04	–	–	0.04	0.07	0.06
Total	99.96	99.97	99.97	99.97	99.96	99.95	99.95	99.95
Si	1.96	1.96	1.98	1.98	1.98	1.98	1.99	1.98
Al(IV)	0.04	0.04	0.02	0.02	0.02	0.02	0.01	0.02
Al(VI)	0.02	0.04	0.02	0.05	0.02	0.03	0.01	0.01
Ti	0.01	–	–	–	–	0.01	–	–
Fe^{3+}	–	–	–	–	–	–	0.02	0.02
Fe^{2+}	0.37	0.40	0.40	0.38	0.35	0.33	0.36	0.36
Mn	0.01	–	–	–	–	0.01	0.01	0.01
Mg	0.66	0.63	0.62	0.65	0.68	0.69	0.66	0.67
Ca	0.93	0.91	0.95	0.89	0.93	0.90	0.90	0.90
Na	0.02	0.03	0.01	0.02	0.04	0.05	0.04	0.05
K	–	–	–	–	–	–	–	–
Jd, %	1.9	2.9	1.4	2.1	4.0	4.5	2.3	3.4
X_{Fe}	0.36	0.39	0.39	0.37	0.34	0.33	0.35	0.35

between garnet and clinopyroxene in this domain during an intermediate retrograde stage.

For a garnet grain from Sample MF-320, a temperature of 665°C was determined for the garnet core (Powell, 1985) and 640°C for the margin with retrograde zoning.

Metabasites of Type II

According to the *Grt–Hbl* thermometer of Powell (1985), the crystallization temperature of the outermost garnet zone with prograde zoning in Sample GMMF-2 (Fig. 5) is 699°C for one of its margins and 648°C for another one. An earlier-stage temperature in the core of the garnet grain is 601°C.

For a garnet from Sample GMMF-B with a nearly homogeneous inner part, the temperature of an early, pre-culmination stage was determined to be 646°C, and that for a marginal retrograde zone, it is 662°C.

The pressure at the culmination of the prograde metamorphism was evaluated by the *Grt–Hbl–Pl–Qtz* barometer at 8.2–8.8 kbar (Kohn and Spear, 1990).

Hence, the **maximum** estimated *P–T* parameters for the peak of the prograde metamorphism in the garnet–clinopyroxene metabasites are as follows: 705°C for the rocks of type I, 699°C and 8–9 kbar for the rocks of type II. According to the *Cpx–Ab–Qtz* barometer (Holland, 1980), metabasites with clinopyroxene containing no more than 7% *Jd* should crystallize, at $T \sim$ 700–750°C at P no lower than 6–8 kbar. Hence, the crystallization temperature of the *Grt–Cpx–Pl–Qtz* matrix of the type-I and -II metabasites are identical, and the pressures are very similar. The cores of progradely zoned garnet crystals (which contain armored clinozoisite relics) yield an early-stage metamorphic tempera-

Table 7. Microprobe analyses of hornblende and plagioclase from the matrix, symplectite, and retrograde reaction rims of garnet–clinopyroxene–amphibole–plagioclase metabasites of types I and II

Component	Matrix			Matrix and symplectite			Matrix		Matrix and symplectite			Retrograde rims of pale green *Hbl*² around *Cpx* and *Hbl*¹			
	*Hbl*¹						*Pl*¹					MF-310			GMMF-B
	MF-310		MF-320	GMMF-2		GMMF-B	MF-310	MF-320	GMMF-2	GMMF-B					
	62	63	64	65	66	67	68	69	70	71	72	73	74	75	76
SiO_2	43.61	43.14	44.41	44.66	45.65	46.42	49.09	55.68	60.05	62.17	61.62	47.55	46.07	49.80	47.29
TiO_2	1.50	1.68	1.66	1.53	1.54	1.31	–	–	–	–	–	0.80	0.77	0.83	0.92
Al_2O_3	11.97	12.10	11.11	10.90	10.13	8.47	32.42	27.96	24.90	23.11	23.75	8.58	9.47	8.23	7.82
FeO	17.44	17.49	17.08	17.27	16.75	18.02	–	0.03	0.17	0.24	0.33	16.56	16.23	16.29	17.09
MnO	0.13	0.09	0.16	0.20	0.12	0.14	–	–	–	–	–	–	0.12	0.20	0.20
MgO	9.43	9.53	9.77	10.11	10.49	10.60		–	0.08	–	0.09	11.35	11.72	11.30	11.30
CaO	11.62	11.66	11.94	11.46	11.50	11.41	15.31	10.23	6.02	4.47	5.12	12.07	11.53	11.90	11.22
Na_2O	1.50	1.02	1.28	1.45	1.31	1.34	2.79	5.95	8.54	9.84	8.95	0.90	1.08	0.74	1.37
K_2O	0.95	1.06	0.96	0.78	0.73	0.57	0.01	0.05	0.08	0.10	0.12	0.09	0.66	0.59	0.49
Total	98.15	97.77	99.80	98.36	98.22	98.28	99.63	99.90	99.84	99.69	99.98	97.90	97.65	97.88	97.70
Si	6.47	6.41	6.58	6.58	6.71	6.28	2.24	2.51	2.68	2.76	2.73	6.95	6.74	7.14	6.95
Al(IV)	1.53	1.59	1.42	1.42	1.29	1.17	1.75	1.48	1.31	1.21	1.25	1.05	1.26	0.86	1.05
Al(VI)	0.56	0.53	0.52	0.47	0.46	0.30						0.43	0.37	0.53	0.30
Ti	0.17	0.19	0.18	0.17	0.17	0.14	–	–	–	–	–	0.09	0.08	0.09	0.10
Fe^{3+}	0.14	0.23	0.08	0.21	0.16	0.23	–	–	–	–	–	0.19	0.33	0.08	0.25
Fe^{2+}	2.02	1.94	2.04	1.92	0.89	1.98	–	–	0.01	0.03	0.01	1.83	1.65	1.87	1.85
Mn	0.02	0.01	0.02	0.02	0.01	0.02	–	–	–	–	–	–	0.01	0.02	0.02
Mg	2.09	2.11	2.16	2.22	2.30	2.32	–	–	–	–	0.01	2.47	2.55	2.41	2.47
Ca	1.85	1.85	1.90	1.81	1.81	1.80	0.74	0.49	0.29	0.21	0.24	1.89	1.81	1.83	1.77
Na	0.43	0.29	0.37	0.41	0.37	0.38	0.25	0.52	0.74	0.85	0.77	0.25	0.31	0.21	0.39
K	0.18	0.20	0.18	0.15	0.14	0.11	–	0.01	–	0.02	0.01	0.02	0.12	0.11	0.09
X_{Fe}	0.51	0.51	0.50	0.49	0.47	0.49						0.45	0.44	0.45	0.46
An, %							75.2	48.6	28.2	20.0	23.9				

ture of 600–630°C, and the retrograde outer rims, which reflect the termination of exchange reactions in the *Grt–Cpx* and *Grt–Hbl* pairs during cooling, gave temperatures of 640–660°C. This apparently demonstrates that the metamorphic parameters remained the same in the metabasites of types I and II during the prograde and retrograde stages.

An additional argument demonstrating that the maximum temperature of the metamorphic culmination did not exceed 700 °C is the important fact that the garnet preserves its prograde zoning. Pressure values of no higher than 8–9 kbar are, in turn, corroborated by the very low jadeite solubility in the clinopyroxene (no more than 4.5%). The occurrence of progradely zoned garnet in the high-temperature Malá Fatra Mts. metabasites is readily explainable, because such garnets are sporadically found even in granulite-facies rocks (Chen *et al.*, 1998), which is explained by the very brief duration of the peak metamorphic conditions.

The estimated metamorphic temperature of the garnet–clinopyroxene metabasites of 700°C coincides with earlier estimates for the metamorphism of sillimanite–garnet gneisses of the Malá Fatra Mts. Complex, which host the amphibolites (Korikovsky *et al.*, 1987). It is interesting to mention that these aluminous gneisses bear preserved armored staurolite relics inside plagioclases, a fact that corresponds to the presence of armored epidote relics in the amphibolite, and points to a common prograde trend of metamorphism for all of the rocks. Our estimates are somewhat lower than the values of 700–750°C, obtained for the metabasites and gneisses of Malá Fatra Mts. by Janák and Lupták (1997). At the same time, our pressure estimates are very close to those of Janák and Lupták (1997) and are 8–10 kbar.

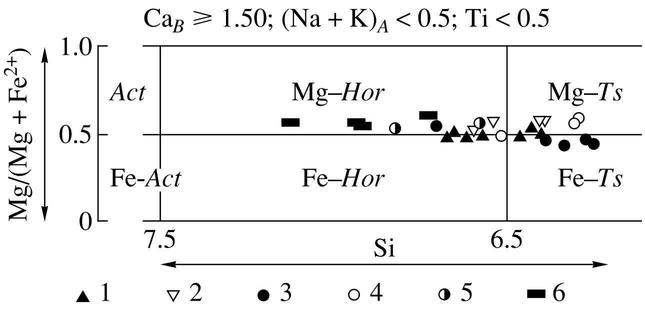

Fig. 7. Compositions of Ca-amphibole from *Grt–Cpx–Hbl–Pl* ± *Qtz* amphibolite, plotted in the diagram by Leake *et al.* (1997).

(1–2) Type-I rocks: (1) crystals from the matrix, (2) inclusions in garnet; (3–5) type-I rocks: (3) from *Pl–Hbl* rims around *Grt*, (4) inclusions in *Grt*, (5) from *Cpx–Pl–Hbl–Ttn* symplectites and the matrix, (6) the youngest pale green amphibole from reaction rims around *Cpx* and *Hbl*[1].

GENESIS OF THE GARNET–CLINOPYROXENE METABASITES AND THEIR PHASE EQUILIBRIA

The garnet–clinopyroxene metabasites in the Malá Fatra Mts. crystalline complex were first described by Hovorka *et al*. (1992), and their genesis was later discussed by Janák *et al*. (1997) and Janák and Lupták (1997). The main conclusion inferred from the occurrence of clinopyroxene–plagioclase symplectites was that the rocks are retrogradely recrystallized eclogites, whose symplectites developed in place of omphacite during the exhumation of the rocks. However, this conclusion is applicable only to the metabasites of type II, because the rocks of type I bear no symplectites. Our newly obtained mineralogical data and paragenetic observations call for the revision of earlier ideas.

Disregarding the symplectitic textures, the occurrence of garnet–clinopyroxene–plagioclase metabasites and amphibolites with clinopyroxene containing no more than 1–7% *Jd* (Hovorka and Méres, 1990; Spišiak and Pitoňák, 1990; Janák *et al.*, 1977) in the Malá Fatra Mts. and other complexes of the Western Carpathians suggests that pressures were no higher than 8–9 kbar, which is confirmed by *Grt–Hbl–Qtz* and *Cpx–Pl–Qtz* geobarometry. Pressure estimates for well-known metamorphic complexes worldwide that were produced at T = 700–750°C and contain the *Grt–Cpx–Pl–Qtz* assemblage with similarly low-Na *Cpx* (for example, amphibolites of the Mica Creek Complex, the Eastern Dalradien metabasites, Ontario region, and others) vary over the same interval of medium pressures: 6–8 kbar (Ghent *et al.*, 1983; Baker, 1985; Percival, 1983; Pattison and Newton, 1989; Ai, 1994; Liu, 1998). Hence, our pressure estimates of 8–9 kbar for the Malá Fatra Mts. Complex practically do not extend outside the overall range of parameters characteristic of *Grt–Cpx* rocks of the amphibolite facies with Na-poor clinopyroxene.

Now, let us consider more closely the phase relations and mineralogy of the rocks of types I and II that can provide a clue for their genesis.

Garnet–Clinopyroxene Metabasites of Type I

The garnet–clinopyroxene metabasites of type I show usual evidence of one-stage metamorphism, because they contain no reaction symplectites with *Cpx*, *Hbl*, and *Pl* and no omphacite relics. These are coarse-grained granoblastic rocks, with Ca-rich plagioclase, and nearly Na-free augite. They contain garnet with preserved prograde zoning in the cores or even throughout its crystals, and thin retrograde rims. Data of *Grt–Cpx* thermometry of the garnets from cores to rims confirm the one-stage prograde character of the metamorphism with the retrograde recrystallization of the outermost portions of garnet crystals during the exhumation and cooling stage. The prograde character of metamorphism is corroborated by the development of titanite rims around rutile and ilmenite: according to the experimental data of Manning and Bohlen (1991, Fig. 2B), rutile in association with zoisite and plagio-

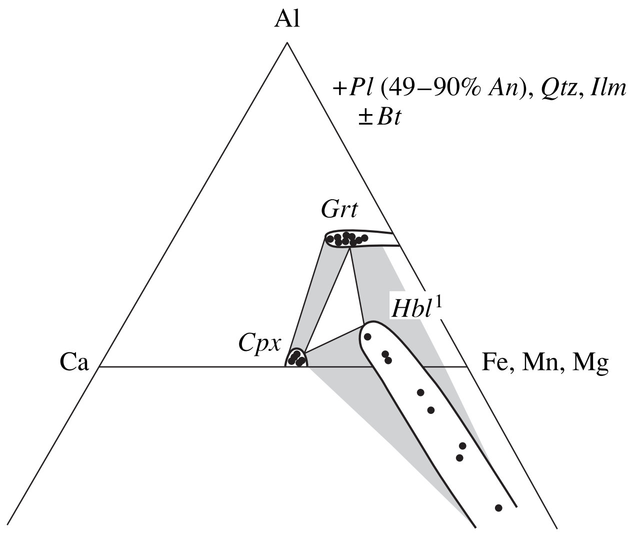

Fig. 8. Phase equilibria in coarse-grained *Grt–Cpx–Hbl–Pl–Qtz* metabasites of type I (Samples MF-310 and MF-320). A projection from the point of coexisting *Pl*: *Pl* (80% *An*) for Sample MF-310 and *Pl* (50% *An*) for Sample MF-320.

clase at, for example, $P \sim 8$–9 kbar and $T > 660$°C should be replaced by titanite with increasing temperature. This is supplementary evidence for the prograde trend of metamorphism of the type-I metabasites, which was inferred from the study of the garnet.

Figure 8 demonstrates the compositions of minerals and phase relations in the type-I metabasites as a projection from the point of calcic plagioclase. The configuration of the tie-lines in the ACF plot readily explains the equilibrium coexistence of lenses of *Aug–Grt–Hbl–Pl* rocks with the surrounding common *Aug-* and *Grt*-free amphibolites by the effect of the bulk-rock composition of the metabasites. It follows from the diagram that clinopyroxene and garnet crystallized only in Ca- and Al-enriched rocks, i.e., in lenses of type-I metabasites, whereas in metabasites with an average or low (Ca + Al)/(Mg + Fe) ratio, only amphibole can be produced, i.e., common plagioclase amphibolite without garnet and clinopyroxene. Moreover, the crystallization of such a ferrous mineral as garnet requires a high bulk-rock X_{Fe} value. Hence, the difference of the type-I metabasites from other rocks is their richness in Ca, Al, and Fe as compared with other amphibolites.

An analogous dependence of the stability of *Cpx* and *Grt* on the (Ca + Al)/(Mg + Fe) ratio in amphibolite-facies metabasites was also established for other areas (Begin, 1992) and is far from unusual. Furthermore, the equilibrium coexistence, at $P > 6$ kbar, of *Grt–Cpx* metabasites and plagioclase amphibolites, a process that depends exclusively on the chemistry of the rocks, was described as proceeding at $P > 6$ kbar not only in the amphibolite facies (Ghent *et al.*, 1983; Baker, 1985; Percival, 1983) but also in the granulite facies. Under the latter conditions, amphibolites can be isofacial even with two-pyroxene–plagioclase gneisses only because both rock types are derived from protoliths of different chemical composition, for example, with different Si concentrations (Auwera, 1993).

Garnet–Clinopyroxene Metabasites of Type II

Genesis of *Cpx–Pl–Hbl–Ttn* symplectites. Let us now turn to the much disputable problem of the genesis of symplectite- and kelyphite-bearing metabasites of type II, which are considered to be either former eclogites (Hovorka *et al.*, 1992, 1994, 1997; Janák *et al.*, 1997) recrystallized under overprinted amphibolite-facies conditions or the products of a single amphibolite-facies metamorphic event, as are the type-I metabasites.

The main argument put forth in support of eclogite recrystallization is the finds of omphacite relics. Had the recrystallization been complete, omphacite relics would have been encountered, at least sporadically, in the form of armored relict inclusions in garnet, which must also have contained relics of Na- and Na–Ca-amphiboles, persistently present in eclogites. The garnet itself would have retained relict more magnesian, “high-pressure” cores and acquired retrograde zoning during the pressure decrease. These are exactly the indications that are traditionally employed (all or only some of them) as evidence in support of a high-pressure stage in polycyclic metamorphic complexes.

Hence, the problem is whether such lines of evidence have ever been encountered in the Malá Fatra Mts. metabasites of type II. In spite of exhaustive studies, no omphacite relics were ever detected in any sample, and no armored omphacite or Na- and Na–Ca-amphibole relics were encountered in the garnet, whose crystals are also devoid of magnesian cores. Conversely, all examined garnets have more ferrous cores, clear prograde zoning with a thin retrograde rim, and the armored inclusions are common hornblende, acid plagioclase, and epidote but not high-pressure minerals. All these facts definitely indicate that the metamorphism evolved progradely during the growth of the garnet, and, judging from the composition of inclusions, *the early metamorphic stage corresponded to the ordinary epidote amphibolite*, but not eclogite facies, with totally stable acid plagioclase.

Practically the only argument that remains in support of the early eclogite metamorphic stage is the occurrence of *Cpx–Pl–Hbl* symplectites, which are commonly regarded as traces of omphacite decomposition (Joanny *et al.*, 1991), although it was definitely established that they can be produced by other mechanisms (Korikovsky *et al.*, 1997). Let us now consider more closely some distinctive features of the *Cpx–Pl–Hbl* ± *Ttn* symplectites in the type-II Malá Fatra Mts. metabasites, which are notably different from analogous symplectites in proved eclogites.

First, as was mentioned above, no omphacite relics occur in the symplectites. The symplectites themselves are not bimineralic, *Cpx–Pl*, in composition, which is a characteristic feature of pseudomorphs after omphacite (Rubie, 1990; O'Brien *et al.*, 1992; O'Brien, 1993; Medaris *et al.*, 1995; Peacock and Goodge, 1995; Liati and Seidel, 1996; Arenas *et al.*, 1997; Markl and Bucher, 1997; Oberhansli *et al.*, 1997), and contain single crystals of high-temperature brown–green hornblende (Table 7) and tiny newly formed titanite crystals. A striking and very unusual feature of the symplectites is the occurrence of large crystals of primary hornblende within them, whose margins show evidence of replacement by symplectite (Figs. 3a, 3b). This feature indicates that the large amphibole crystals are older than the symplectite, which grows by the resorption of this mineral (among others).

Second, the composition of augite in the symplectite is also unusual. In true eclogites, omphacite is replaced by *Cpx–Pl* symplectite, whose *Cpx* is lower in *Jd* than the primary omphacite, and whose *Jd* concentration widely varies in the course of the long-lasting exhumation. For example, in eclogites from the Münchberg Massif (O'Brien, 1993), the decomposition of primary omphacite (60–62% *Jd*) produces *Cpx–Pl* symplectite with Cpx^2 with 45–7% *Jd*. In the eclogites of the Ordenes Complex (Arenas *et al.*,1997), newly-formed symplectites at the sacrifice of omphacites with up to 40% *Jd* contain Cpx^2 with 31–7% *Jd*. Conversely, symplectites in the Malá Fatra Mts. type-II metabasites bear augite of practically uniform, Na-free composition with 1–4% *Jd*. These constant compositions of Cpx^2 are absolutely atypical of true eclogites. The textures of the Malá Fatra Mts. symplectites is also different: it is not only dactylitic or symplectitic but also normal microgranoblastic but never globular, which is characteristic only of pseudomorphs after round omphacite crystals (Joanny *et al.*, 1991).

Third, in the type-II metabasites, fine-grained *Cpx–Hbl–Pl* symplectite alternates with a medium- or coarse-grained *Hbl–Pl* ± *Ilm* matrix (Figs. 3a, 3b) with 40–50% *Pl*. This nematogranoblastic-granular matrix is undoubtedly primary and exhibits no evidence of development at the expense of some high-pressure minerals, as could be expected if it developed after eclogite during decompression.

Hence, even symplectites in the type-II metabasites show unusual features, which do not confirm their development by the decomposition of omphacite, and their genesis requires other explanations. They are most similar to analogous textures in the high-pressure Ograzhden amphibolite–gneiss complex in Macedonia (Korikovsky *et al.*, 1997).

When studying garnet amphibolites in the Ograzhden Complex, Macedonia, Korikovsky *et al.* (1997) determined that *Cpx–Pl* symplectites had been produced in these rocks by the resorption of hornblende and clinozoisite due to the prograde reaction $Hbl^1 + Czo + Qtz = Cpx^2 + \{Ab–Olg^2\} + Grt(\mathrm{rim}) + H_2O$. The symplectites bear armored relics of both hornblende and clinozoisite, along with newly formed crystals of titanite, and the coexisting garnet displays well-pronounced prograde compositional variations even in the outermost rims. Very similar prograde symplectites around hornblende and clinozoisite were also found in the eclogite–amphibolites of the Sieggraben Complex in the Eastern Alps (Putiš *et al.*, 2000), in which they are usually formed simultaneously with the compositionally and morphologically similar $Cpx^2–Pl^2$ symplectites around omphacite, because the initial exhumation of the complex was associated with a slight temperature increase.

The total similarity, up to the tiniest details, between the development of symplectites in the amphibolites of the Ograzhden Complex and the type-II rocks from the Malá Fatra Mts., particularly, the occurrence of large crystals of primary hornblende, but not omphacite relics, in the symplectites, led us to suggest that the rocks were produced in a similar manner, by the prograde decomposition of the hornblende and clinozoisite assemblage, but not by the retrograde recrystallization of eclogites. Only this model can explain all of the aforementioned features of these rocks. They may be summarized as follows:

(1) The total absence of omphacite relics in the group-II metabasites;

(2) Prograde zoning of the garnet and the fact that this mineral contains inclusions of usual minerals of the epidote amphibolite facies (Ca-amphibole, clinozoisite, and acid plagioclase), but never high-pressure phases (omphacite and Na- or Na–Ca-amphiboles);

(3) The presence, in the *Cpx–Pl* symplectites, of small, medium, and large crystals of high-temperature hornblende with traces of resorption (which suggest the relict character of the mineral). Its partial decomposition (in the presence of clinozoisite and quartz) resulted in *Cpx–Pl–Ttn* symplectites;

(4) The occurrence, in the symplectites, of tiny crystals of newly formed titanite, which is always produced during the decomposition of Ti-bearing amphiboles but never crystallizes during the breakdown of nearly Ti-free omphacite.

The most realistic scenario for the formation of the symplectites in the type-II metabasites is the following prograde reaction, which resulted in *Cpx–Pl* symplectites in the type-II metabasites:

$$Hbl^0 + Czo^0 + Qtz$$
$$\longrightarrow \{Cpx + Olg\text{-}And\} + Grt(\mathrm{rim}) + Ttn + H_2O.$$

Apparently, this reaction took place during the transition from the epidote amphibolite to amphibolite facies in the crystalline complex of the Malá Fatra Mts. The reaction can be regarded as the dehydration process and the extension of the clinopyroxene stability field at the expense of the partial decomposition of Ca-

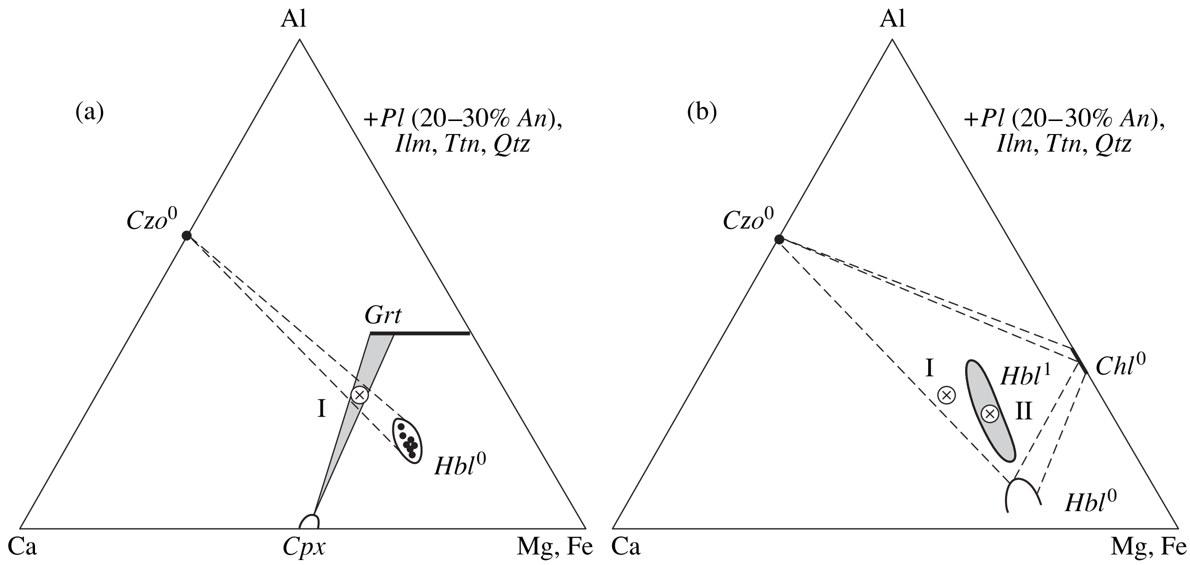

Fig. 9. Graphic interpretation for the proposed prograde metamorphic reactions in (a) type-II metabasites and (b) host plagioclase amphibolites (see text).

(a) Reaction in *Grt*-bearing, slightly Ca-, Al-, and Fe-enriched rocks (point I): $Hbl^0 + Czo^0 + Qtz \longrightarrow \{Cpx + Olg\text{–}And\} + Grt(\mathrm{rim}) + Ttn + H_2O$.

(b) Reaction in *Grt*-free rocks with lower (Ca + Al)/(Mg + Fe) ratio and X_{Fe} value (point II): $Hbl^0_{\mathrm{Al<}} + Czo^0 + Chl^0 + Pl \longrightarrow Hbl^1_{Ts\text{-}Ed\text{-}Prg\text{-}Hst} + Qtz + H_2O$. Projection from the point of *Pl* (30% *An*).

amphibole. The latter remains preserved in symplectites. Clinozoisite is fully consumed during this reaction, disappears from the matrix, and can be encountered only as armored inclusions in garnet. Garnet, which is one of the reaction products, grew in the form of an outer prograde rim around earlier garnet. Titanite forms small euhedral crystals. The constant composition of Cpx_2 can be explained only by the development of symplectites at the metamorphic culmination, but not retrogression, because only culmination assemblages exhibit the strongest tendency toward equilibrium.

Similar *Cpx*-forming reactions, which are associated with the breakdown of the hornblende–epidote assemblage but not the development of symplectitic textures, were detected in, for example, amphibolite-facies rocks in Massachusetts (Schumacher, 1991).

An important problem that should be accounted for within the guidelines of this model is the possible reasons for the development of *Cpx–Pl–Ttn* symplectites after amphibole and clinozoisite only in lenses and boudins of the type-II amphibolites but not in the neighboring amphibolites. This is most probably explained by the primary bulk-rock compositional differences between these rocks and, as a consequence, different prograde reactions in them.

The type-II metabasites are enriched in Ca, Al, and Fe (although this enrichment is not as strong as in the type-I metabasites), as follows from the presence of Ca–Fe–Al minerals, such as garnet with clinozoisite inclusions. This means that the $Hbl^0 + Czo^0$ assemblage (Fig. 9a, composition I) was stable in the earlier epidote amphibolite facies, and its breakdown during the transition to the amphibolite facies resulted in *Cpx–Pl–Ttn* symplectites and prograde garnet margins in accordance with the aforementioned reaction.

The surrounding plagioclase amphibolites of the leptinite–amphibolite complex contain no garnet, which points, according to Fig. 8, to their lower (Ca + Al)/(Mg + Fe) ratio and lower X_{Fe} (Fig. 9b, composition II). Under amphibolite-facies conditions, the rocks could contain the stable $Hbl^0 + Czo^0 + Chl^0$ assemblage (which is typical of this facies) with chlorite instead of Fe–Ca–Mg garnet and with low-Al amphibole. The breakdown of this assemblage during the transition to the amphibolite facies (Fig. 9b) gave rise to more aluminous Ca-amphiboles of tschermakitic, pargasitic, or hastingsitic composition. This process was, perhaps, associated with an increase in the *An* concentration in the plagioclase due to clinozoisite decomposition by the reaction

$$Hbl^0_{\mathrm{Al<}} + Czo^0 + Chl^0 + Pl \longrightarrow Hbl^1_{Ts\text{-}Ed\text{-}Prg\text{-}Hst} + Qtz + H_2O.$$

This reaction led to the full disappearance of clinozoisite and chlorite, and the epidote-chlorite amphibolites were transformed into normal plagioclase amphibolites without *Cpx* and *Grt*. Hence, even relatively insignificant differences in the Ca : Al : (Mg + Fe) proportions between the metabasites (compare compositions I and II in Fig. 9) affects the mineral assemblages of the high-temperature rocks during the transition from the epidote amphibolite to amphibolite facies.

In comparing the metabasites of types I and II, their similar prograde geneses can be inferred from the similarities between the compositions of their mafic rock-forming minerals:

(a) The ferrous composition of all garnets, which differ only by grossular concentrations and have similar prograde or prograde–retrograde zoning;

(b) Similar and very low *Jd* concentrations (1–4%) in all clinopyroxenes with similar X_{Fe} values (0.34–0.39);

(c) The affiliation of all high-temperature Ca-amphiboles to a single low-Na hornblende–tschermakite series (*Hb–Ts*) with analogous X_{Fe} (~0.50).

Such a total similarity is possible only at the similar metamorphic parameters of the metabasites of both types. This is confirmed by the identity of the maximum temperature estimates (~700°C), in spite of slight differences in the Ca and Al concentrations in the protoliths (see above).

This interpretation makes it possible to explain not only similarities but also the differences between the stability and morphology of clinopyroxene in the type-I and type-II rocks. If type-I rocks were higher in Ca and are calc-silicate rocks (see above), their clinopyroxene should have appeared under the conditions of the previous epidote amphibolite facies, probably, at the sacrifice of Fe–Mg–Ca carbonates (Spear, 1995), and, because of this, clinopyroxene occurs not only in the matrix of these rocks but also in the form of inclusions in "low-temperature" progradely zoned garnet cores, which contain, in addition to this mineral, inclusions of clinozoisite. The metabasites of type II are poorer in Ca and, thus, their *Cpx*-forming reactions started to proceed at a higher temperature, only at the metamorphic peak. This fact explains the presence of *Cpx* only in the matrix of these rocks and in their newly formed *Cpx–Pl–Ttn* symplectites and the absence of *Cpx* among inclusions in the garnet.

The processes of prograde hornblende decomposition observable in thin sections, and the resorption and armoring of this mineral by *Cpx–Pl* or *Opx–Cpx–Pl* matrix or symplectites are far from unusual phenomena in metabasites not only of the amphibolite but also of the granulite facies (Stoddard, 1985; Hollocher, 1991; Russ-Nabelek, 1989; Todd and Evans, 1994).

Genesis of doubled *Pl–Hbl* kelyphitic rims around garnet. In addition to *Cpx–Hbl–Pl–Ttn* kelyphites, the type-II metabasites bear unusual concentric kelyphites around garnet at its contacts with *Cpx*-bearing symplectites or with the matrix (Figs. 3a, 3c). The symplectites consist of an inner nearly monomineralic plagioclase rim (with rare hornblende crystals) and an outer, hornblende-rich rim (with oligoclase inclusions). Garnet crystals surrounded by these rims retain their prograde zoning (Fig. 5), the plagioclase in the rims (as well in the matrix and the symplectites) is oligoclase–andesine, and the hornblende in the inner and outer zones of the kelyphites has a brown–green color, and its composition is the same as the composition of all high-temperature hornblendes in the rocks of types I and II (Tables 2–5, 7, Fig. 7). The amphibole in the outer parts of the kelyphites, in contact with the adjacent matrix or symplectite, often occurs in reaction relationships with small augite crystals in the matrix (symplectite), and fully or partly replaces them (Fig. 3c). In turn, crystals of kelyphitic hornblende are sometimes replaced in the margins by retrograde pale green amphibole (Table 7, Fig. 7). This fact suggests that the kelyphitic rims themselves developed prior to the retrograde stage. Hence, it can be stated that the concentric *Pl–Hbl* rims were formed somewhat later than the *Cpx–Pl–Hbl–Ttn* symplectites but earlier than medium-temperature retrograde processes were initiated.

Before discussing the genesis of the *Pl–Hbl* kelyphites in the type-II metabasites, let us turn to their analogues in some *Cpx–Grt* metamorphic rocks described in the literature. *Hbl–Pl* rims develop in these rocks not just around garnet crystals, but necessarily at their contacts with clinopyroxene. For example, natural eclogites commonly carry bimineralic *Hbl–Pl* kelyphites with a symplectitic texture, which surround garnet at its physical contacts with omphacite (Messiga *et al.*, 1992; Markl and Bucher, 1997; Korikovsky *et al.*, 1997). The ratio of *Hbl* and *Pl* ranges in them from 8 : 2 to 1 : 1. The origin of these rims is usually believed to result from the "garnet–omphacite reaction" (Carlson and Johnson, 1991), which marks the onset of the breakdown of the *Grt* + *Omp* assemblage in response to exhumation-related decompression.

However, absolutely analogous *Hbl–Pl* rims around garnets also develop during the breakdown of the *Cpx–Grt* assemblage in the course of exhumation of ordinary garnet–clinopyroxene–plagioclase metabasites metamorphosed at P ~ 6–9 kbar. For example, in the subgranulite Labrador Complex (Mengel and Rivers, 1991), garnet–plagioclase rocks with augite containing 3–5% *Jd*, the *Hbl–Pl* symplectites develop at *Grt* ± *Cpx* contacts as a consequence of decompression. Simultaneously, the garnet acquires retrograde zoning, which, along with geothermobarometric data, points to a simultaneous decrease in P and T during the development of the rims in this complex.

A somewhat different morphological type of *Hbl–Pl* reaction rims, which, however, amazingly resemble the *Hbl–Pl* reaction rims in the Malá Fatra Mts. type-II metabasites, was documented in the *Grt–Cpx–Pl–Qtz* amphibolites of Geticum (Korikovsky *et al.*, 1993). The garnet of the rocks preserves its clear-cut prograde zoning and is surrounded by doubled kelyphites in contacts with the *Cpx–Pl–Hbl* matrix. The inner parts of the kelyphites consist of oligoclase, and their outer por-

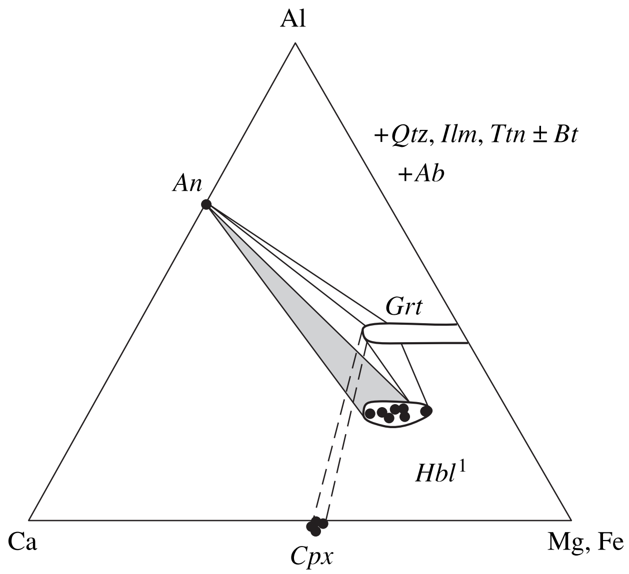

Fig. 10. Graphic interpretation for the development of doubled *Hbl* and *Pl* rims around *Grt* crystals by the reaction *Grt* + *Cpx* + Na_2O + H_2O ⟶ *Hbl* + *Pl* (20–40% *An*) + *Qtz* in metabasites of type II (Samples GMMF-2 and GMMF-B). Projection from the *Ab* point.

tions are made up of hornblende. The striking similarities between the reaction textures in metabasites of the Malá Fatra Mts. and Geticum is amplified by the compositional closeness of the minerals: clinopyroxene in the matrix of the Geticum rocks contains 2–7% *Jd*, and the progradely zoned garnet have X_{Fe} from 0.86 in the cores to 0.69–0.77 in the margin at grossular concentrations from 31 to 23%. Contrary to the zoning of garnet from Labrador complexes (Mengel and Rivers, 1991), the prograde zoning of kelyphitized garnet from the Geticum metabasites indicates that their uplift did not begin with a temperature decrease but with its slight increase (or a constant value).

Let us return to the type-II metabasites from Malá Fatra Mts. The development of their *Pl–Hbl* kelyphites around garnet exclusively at contacts with *Cpx*-bearing symplectites or the matrix of the same composition (Figs. 3a, 3c) indicates that they were produced, as in the cases discussed above, by a reaction between garnet and symplectitic (or matrix) clinopyroxene (Fig. 7) early in the decompression stage. The formation of the kelyphites very close to the metamorphic culmination is confirmed by the preservation of prograde zoning in the kelyphitized garnet, the same amphibole and plagioclase types in kelyphites and symplectites in the type-II metabasites (Fig. 7), and the identity of the maximum temperature estimates for the kelyphitized type-II metabasites (Table 4) and the type-I metabasites (Table 2).

The kelyphite-forming reaction (Fig. 10), which is isochemical in terms of Ca, Al, and (Mg, Fe), was apparently coupled with, and stimulated by, Na influx, because the newly formed *Hbl* + {*Olg–And*} assemblage is much higher in Na than the primary *Grt* + *Cpx* association. Hence, the process can be expressed by the reaction

$$Grt + Cpx_{\text{Na-poor}} + Na_2O + H_2O$$
$$\longrightarrow Pl(20\text{–}40\%\ An) + Hbl \pm Qtz.$$

Sodium inflow at temperatures close to the metamorphic culmination during initial decompression is most probably coeval with migmatization, partial melting, and the development of tonalites in the high-temperature Malá Fatra Mts. Complex (Janák *et al.*, 1995). Such processes are usually accompanied by the active migration of alkalies. The absence of such *Pl-Hbl* kelyphites in the type-I metabasites is explained by the fact that they were most probably not affected by Na metasomatism, as can be inferred from the stability of calcic plagioclase (80–87% *An*, Table 2) in these rocks.

This provokes the question as to why decompression-related reaction textures between garnet and augite are different, and why *Grt–Cpx–Pl* metabasites sometimes contain *Pl–Hbl* kelyphites with a symplectitic texture, in which small *Pl* and *Hbl* crystals are contained in an approximately 1 : 1 proportion (Mengel and Rivers, 1991), and sometimes, as in the Geticum (Korikovsky *et al.*, 1993) and Malá Fatra Mts. complexes, the rocks contain concentrically zoned kelyphites composed of zones with sharp contacts (plagioclase and hornblende), although the integral bimineralic compositions of the rims is the same in both cases. Evidently, the inner structure of such bimetasomatic rims depends on kinetic factors (Korzhinsky, 1970), particularly, on the counterdiffusion rates of components between reacting minerals: clinopyroxene and garnet. Studying corona *Grt–Cpx–Opx* textures in metagabbro, which have been produced by reactions between crystals of olivine and plagioclase and consisted of concentric monomineralic zones (*Ol* ⟷ *Opx* ⟷ *Cpx* ⟷ *Grt* ⟷ *Pl*), Grant (1988) determined that the main factor controlling the inner structures of such rims is the relative diffusion rates of components. The most inert and the least mobile component of coronites is Al, and the rate of counterdiffusion increases in the succession Al ⟶ Ca ⟶ Mg. Variations in these rates in distinct domains with the same composition of reacting olivine and plagioclase predetermined the differences in the internal structure and composition of the coronal rims. In particular, the inert behavior of Al and the high mobility of Mg explain the fact that such an Al-rich phase as garnet composes a monomineralic corona on the side of plagioclase, whereas monomineralic orthopyroxene rim (which is Al-free) develops on the side of olivine.

Apparently, the diffusion-controlled mobility of components in the Malá Fatra Mts. metabasites determined the structure of the *Pl–Hbl* rims during the reaction between garnet and augitic clinopyroxene in the adjacent symplectite or matrix. If the mobility of Al is much lower than those of Mg and Fe, this facilitates the crystallization of a nearly monomineralic oligoclase–andesine rim with small amounts of hornblende crystals around such Al-rich phase as garnet, and the development of nearly monomineralic hornblende rim with subordinate amounts of oligoclase on the side of the *Cpx*-bearing symplectite or matrix. To put it otherwise, the assemblage developing adjacent to garnet has a very high Al/(Mg + Fe) ratio, whereas the assemblage near clinopyroxene is characterized by a low ratio. This succession of zones (*Grt* ⟷ *Pl* ⟷ *Hbl* ⟷ *Cpx*) is shown in Fig. 10 as a projection from the point of *Ab* with the actual compositions of the minerals. The causes of the sharpness of boundaries between the plagioclase and hornblende zones and of the almost monomineralic composition of these zones can be readily accounted for by the theory of metasomatic zoning (Korzhinskii, 1970).

Provided the diffusion rates of Al, Mg, and Fe become closer to one another for a variety of reasons, a homogeneous bimineralic symplectitic *Hbl–Pl* rim develops between the garnet and augite, with the amounts of *Pl* and *Hbl* ingrowths varying around the ~1 : 1 ratio. This can be exemplified by the aforementioned *Hbl–Pl* symplectites in the *Grt–Cpx–Opx–Pl* metabasites of the Labrador Complex (Mengel and Rivers, 1991) and, perhaps, also the *Hbl–Pl* symplectites around garnet in the *Grt–Cpx* metabasites from the Tatra Mountains (Janák *et al.*, 1996; Fig. 3b), if their origin can be described by the same model as that for the Malá Fatra Mts. metabasites. The latter seems to be highly probable, given the fact that the *Hbl–Pl* symplectites of the metabasites were also formed along contacts between garnet (which retains its prograde zoning) and *Cpx–Pl* symplectites, in which augite crystals contain no more than 5% *Jd*, and relics of earlier omphacite are completely absent.

CONCLUSION

1. The garnet–clinopyroxene metabasites that occur as lenses among amphibolites of the Malá Fatra Mts. crystalline complex can be classified into two groups, which differ in texture and in the presence or absence of symplectitic and kelyphitic rims but are similar in the composition of minerals.

2. Type I comprises coarse-grained equilibrium *Grt–Aug–Hbl–Pl–Qtz* rocks without symplectites or kelyphites, with progradely zoned garnet (having a thin retrograde rim), augite with no more than 4% *Jd* (in the matrix and inclusions in garnet), calcic plagioclase (49–87% *An*), and brown–green hornblende. These rocks display all typical features of their prograde metamorphic formation: according to the *Grt–Cpx* thermometer, the temperature increased from the cores to rims of garnet crystals from 630 to 705°C and decreased again to 640°C during the development of the outer retrograde rim.

3. Type II includes medium-grained rocks with a matrix of alternating fine-grained *Hbl–Aug* (1–4% *Jd*)–*Pl* (20–40% *An*) ± *Qtz* and medium- to coarse-grained *Hbl–Ilm–Pl* ± *Qtz* material, garnet crystals with prograde zoning and thin retrograde rims, and with reaction textures of two types: fine-grained *Aug* (1–4% *Jd*)–*Pl*(20–40% *An*)–*Hbl–Ttn* symplectites and doubled *Hbl–Pl* kelyphitic rims around garnet at its contacts with symplectites. No omphacite relics were detected either in the symplectites or among inclusions in the garnet. The latter mineral contains inclusions only of common hornblende, epidote, and sodic plagioclase, i.e., minerals of the epidote amphibolite facies. Based on the absence of omphacite relics, the results obtained on the garnet and inclusions in it, the similarities between the compositions of minerals of the type-I and II metabasites, and by analogy with other similar complexes, we arrived at the conclusion that the symplectites were produced by the prograde reaction *Hbl* + *Czo* + *Qtz* ⟶ {*Cpx* + *Olg–And*} + *Grt*(rim) + *Ttn* + H_2O, which reflects the extension of clinopyroxene stability at the sacrifice of hornblende and clinozoisite with the transition from the epidote amphibolite to amphibolite facies but not as a consequence of the retrograde recrystallization of the eclogites, as was thought previously. *Grt–Hbl* thermometric data point to a temperature increase from the cores to rims of garnet crystals from 600 to 699°C (at the metamorphic peak) at a maximum pressure of 8–9 kbar (*Grt–Hbl–Pl–Qtz* barometer). Analysis of the internal structures of *Pl–Hbl* kelyphites around garnet crystals points to their origin by means of the reaction *Grt* + *Cpx* (in symplectite or matrix) + Na_2O + H_2O ⟶ *Pl* (20–40% *An*) + *Hbl* + *Qtz*, which occurred early during decompression, at a temperature close to the metamorphic culmination. Reactions of this type proceed only in Ca-, Al, and Fe-rich rocks, i.e., in boudins of the type-II metabasites but not in rocks with lower (Ca + Al)/(Mg + Fe) ratios, i.e., the surrounding amphibolites.

4. We conclude that the complex of banded amphibolites in the Malá Fatra Mts. crystalline complex, which includes lenses of *Grt–Cpx–Hbl–Pl–Qtz* metabasites, was produced by a prograde metamorphism under conditions of the relatively high-pressure (*P* ~ 8–9 kbar) amphibolite facies at a maximum temperature of approximately 700°C. The decompression was initiated under nearly isothermal conditions (the crystallization of *Pl–Hbl* kelyphites) and further proceeded at an evident temperature decrease, as follows from the development of peripheral retrograde rims in some garnet crystals in the type-I and -II metabasites and from the occurrence of reaction medium-temperature minerals, such as pale green amphibole, which replaces (in the form of thin rims) high-temperature amphibole and clinopyroxene.

ACKNOWLEDGMENTS

This study was supported by the Russian Foundation for Basic Research, project no. 99-05-64058, and the Slovak Grant Agency VEGA, no. 1/5124/98.

REFERENCES

Ai, Y., A Revision of the Garnet–Clinopyroxene Fe^{2+}–Mg Exchange Geothermometer, *Contrib. Mineral. Petrol.*, 1994, vol. 115, pp. 467–473.

Arenas, R., Abati, J., Martinez Catalan, J.R., *et al.*, *P–T* Evolution of Eclogites from the Agualada Unit (Orce Nes Complex, Northwest Iberian Massif, Spain): Implications for Crustal Subduction, *Lithos*, 1997, vol. 40, pp. 221–242.

Auwera, J.V., Diffusion Controlled Growth of *Px*-bearing Margins on Amphibolite Bands in the Granulite Facies of Rogaland (SW Norway): Implications for Granulite Formation, *Contrib. Mineral. Petrol.*, 1993, vol. 114, pp. 203–220.

Bagdasaryan, G.P., Gukasyan, R.Kh., Cambel, B., *et al.*, Granitoids of the Malá Fatra and Velká Fatra Mts.: Rb/Sr Isochron Geochronology (Western Carpathians), *Geol. Carpathica*, 1992, vol. 43, pp. 21–25.

Baker, A.J., Pressures and Temperatures of Metamorphism in the Eastern Dalradian, *J. Geol. Soc.* (London), 1985, vol. 142, pp. 137–148.

Begin, N.J., Contrasting Mineral Isograd Sequences in Metabasites of the Cape Smith Belt, Northern Quebec, Canada: Three New Bathogrades for Mafic Rocks, *J. Metamorph. Geol.*, 1992, vol. 10, pp. 685–704.

Carlson, W.D. and Johnson, C.D., Coronal Reaction Textures in Garnet Amphibolites of the Llano Uplift, *Am. Mineral.*, 1991, vol. 76, pp. 756–772.

Carswell, D.A., Eclogites and the Eclogite Facies: Definitions and Classifications, *Eclogite Facies Rocks*, Carswell, D.A., Ed., Glasgow: Blackie, 1990, pp. 1–13.

Chen, N.S., Sun, M., You, Z.D., and Malpas, J., Well-Preserved Garnet Growth Zoning in Granulite from the Dabie Mountains, Central China, *J. Metamorph. Geol.*, 1998, vol. 16, pp. 213–222.

Eckert, J.O., Newton, R.C., and Kleppa, O.J., The Δ*H* of Reaction and Recalibration of Garnet–Pyroxene–Plagioclase–Quartz Geobarometers in the CMAS System by Solution Calorimetry, *Am. Mineral.*, 1991, vol. 76, pp. 148–160.

Ghent, E.D., Stout, M.Z., and Raeside, R.P., Plagioclase–Clinopyroxene–Garnet–Quatrz Equilibria and the Geobarometry and Geothermometry of Garnet Amphibolites from Mica Creek, British Columbia, *Can. J. Earth Sci.*, 1983, vol. 20, pp. 699–706.

Grant, S.M., Diffusion Models for Corona Formation in Metagabbros from the Western Grenville Province, Canada, *Contrib. Mineral. Petrol.*, 1988, vol. 98, pp. 49–63.

Holland, T.J.B., The Reaction Albite = Jadeite + Quartz Determined Experimentally in the Range 600–1200°C, *Am. Mineral.*, 1980, vol. 65, pp. 129–134.

Hollocher, K., Prograde Amphibole Dehydration Reactions during High-Grade Regional Metamorphism, Central Massachusetts, USA, *Am. Mineral.*, 1991, vol. 76, pp. 956–970.

Hovorka, D. and Méres, Š., Relicts of High-Grade Metamorphites in Tatroveporic Crystalline of the West Carpathians, *Mineral. Slov.*, 1989, vol. 21, pp. 193–201.

Hovorka, D., and Méres, Š., Clinopyroxene–Garnet Metabasites from the Tribec Mts. (Central Slovakia), *Mineral. Slov.*, 1990, vol. 22, pp. 533–538.

Hovorka, D. and Méres, Š., Pre-Upper Carboniferous Gneisses of the Strazóvské Vrchy Upland and the Malá Fatra Mts. (the Western Carpathians), *Acta Geol. Geogr. Univ. Comen. Geology*, 1991, vol. 46, pp. 103–169.

Hovorka, D. and Méres, Š., Leptyno–Amphibolite Complex of the Western Carpathians Occurrences and Lithology, *Mineral. Slov.*, 1993, vol. 25, pp. 1–9.

Hovorka, D., Ivan, P., Jaroš, J., *et al.*, *Ultramafic Rocks of the Western Carpathians, Czechoslovakia*, Bratislava: D. Štur Inst. Geol., 1985, 235 p.

Hovorka, D., Méres, Š., and Cano, F., Petrology of the Garnet–Clinopyroxene Metabasites from the Malá Fatra Mts., *Mineral. Slov.*, 1992a, vol. 24, pp. 45–52.

Hovorka, D.,Méres, Š., and Ivan, P., Pre-Alpine Western Carpathian Mts. Basement Complexes: Geochemistry, Petrology, and Geodynamic Setting, *Terra Abstr., Suppl. no. 2 to Terra Nova*, 1992b, vol. 4, p. 32.

Hovorka, D., Méres, Š., and Ivan, P., Pre-Alpine Western Carpathians Basement Complexes: Lithology and Geodynamic Setting, *Mitt. Österr. Geol. Ges.*, 1994, vol. 86, pp. 33–44.

Hovorka, D., Ivan, P., and Méres, Š., Leptyno–Amphibolite Complex of the Western Carpathians: Its Definition, Extent and Genetic Problems, Grecula, P., Hovorka, D., and Putiš, M., Eds., *Geological Evolution of the Western Carpathians*, Miner. Slov. (Monography), 1997, pp. 269–280.

Ivanov, M. and Kamenický, L., Contributions to Geology and Petrology of the Malá Fatra Crystalline, *Geol. Práce, Zoš*, 1957, vol. 45, pp. 180–216.

Janák, M. and Lupták, B., Pressure–Temperature Conditions of High-Grade Metamorphism and Migmatization in the Malá Fatra Crystalline Complex, the Western Carpathians, *Geol. Carpathica*, 1997, vol. 48, pp. 287–302.

Janák, M., Hovorka, D., Hurai, V., *et al.*, High-Pressure Relics in the Metabasites of the Western Carpathians Pre-Alpine Basement, Grecula, P., Hovorka, D., and Putiš, M., Eds., *Geological Evolution of the Western Carpathians*, *Mineral. Slov.* (Monography), 1997, pp. 301–308.

Janák, M., O'Brien, P.J., Hurai, V., and Reutel, C., Metamorphic Evolution and Fluid Composition of Garnet–Clinopyroxene Amphibolites from the Tatra Mountains, Western Carpathians, *Lithos*, 1996, vol. 39, pp. 57–79.

Janák, M., Pitoňák, P., Spišiak, J., *et al.*, Trondhjemitic–Tonalitic Melts in the Western Carpathians: Implications for Partial Melting of Amphibolite and Differentiation of the Lower Crust, *Terra Nova*, 1995, vol. 7, p. 307.

Joanny, V., van Roemund, H., and Lardeaux, J.M., The Clinopyroxene/Plagioclase Symplectite in Retrograde Eclogites: A Potential Geothermobarometer, *Geol. Rundsch.*, 1991, vol. 80/2, pp. 303–320.

Kamenický, L. and Macek, J., Ein Profil durch die lithostratigraphischen Schichtenfolgen des Kristallinikum des Gebirges Malá Fatra, *Geol. Zborn.—Geol. Carpathica*, 1984, vol. 35, pp. 157–160.

Kohn, M.Y. and Spear, F.S., Two New Geobarometers for Garnet Amphibolites, with Application to Southeastern Vermont, *Am. Mineral.*, 1990, vol. 75, pp. 89–96.

Korikovsky, S.P. and Karamata, S., Garnet–Clinopyroxene Amphibolites from the Geticum Nappe, Eastern Serbia: Metamorphic Evolution and Genesis of Reactional Structures, *Petrology*, 1993, vol. 1, pp. 417–428.

Korikovsky, S.P., Janák, M., and Lupták, B., Phase Relations in Olivine–Orthopyroxene–Chlorite–Spinel–Hornblende Metaultramafics from the Malá Fatra Mts., Western Carpathians, *Geol. Carpathica*, 1998, vol. 49, pp. 369–376.

Korikovsky, S.P., Kamenicky, L., Macek, J., and Boronikhin, V.A., *P–T* Conditions of Metamorphism of the Crystalline Schists in the Malá Fatra (in the Profile of the Mlynsky

Potok Area), *Geol. Zborn.—Geol. Carpathica*, 1987, vol. 38, pp. 409–427.

Korikovsky, S.P., Mirčóvski, V., and Zakariadze, G.S., Metamorphic Evolution and the Composition of the Protolith of Plagioclase-bearing Eclogite–Amphibolites of the Buchim Block of the Serbo–Macedonian Massif, Macedonia, *Petrologiya*, 1997, vol. 5, pp. 534–549.

Korikovskii, S.P., Mircóvski, V., Boev, B., *et al.*, Prograde Formation of Clinopyroxene–Plagioclase Symplectites in Garnet–Clinozoisite Amphibolites of the Ograzhden Complex, Macedonia, *Proc. Symp. Magmatism, Metamorphism, and Metallogeny of the Vardar Zone and Serbo–Macedonian Massif*, Boev, B. and Serafimovski, T., Eds., Štip–Dojran, 1997, pp. 253–256.

Korzhinsky, D.S., *Theory of Metasomatic Zoning*, Oxford: Clarendon, 1970.

Krist, E., Korikovsky, S.P., Putiš, M., *et al.*, *Geology and Petrology of Metamorphic Rocks of the Western Carpathian Metamorphic Complexes*, Bratislava: Univ. Com.,1992, 324 p.

Leake, B.E., Woolley, A.R., and 20 Members of the Subcommittee on Amphiboles, Nomenclature of Amphiboles. Report of the Subcommittee on Amphiboles of the International Mineralogical Association Commission on New Minerals and Mineral Names, *Eur. J. Mineral.*, 1997, vol. 9, pp. 623–651.

Liati, A. and Seidel, E., Metamorphic Evolution and Geochemistry of Kyanite Eclogites in Central Rhodope, Northern Greece, *Contrib. Mineral. Petrol.*, 1996, vol. 123, pp. 293–307.

Liu, J., Assessment of Garnet–Clinopyroxene Thermometer, *Int. Geol. Rev.*, 1998, vol. 40, pp. 579–608.

Manning, C.E. and Bohlen, S.R., The Reaction Titanite + Kyanite = Anorthite + Rutile and Titanite–Rutile Barometry in Eclogites, *Contrib. Mineral. Petrol.*, 1991, vol. 109, pp. 1–9.

Markl, G. and Bucher, K., Proterozoic Eclogites from the Lofoten Islands, Northern Norway, *Lithos*, 1997, vol. 42, pp. 15–35.

Medaris, G., Jelinek, E., and Misař, Z., Czech Eclogites: Terrane Settings and Implications for Variscan Tectonic Evolution of the Bohemian Massif, *Eur. J. Mineral.*, 1995, vol. 7, pp. 7–28.

Mengel, F. and Rivers, T., Decompression Reactions and *P–T* Conditions in High-Grade Rocks, Northern Labrador: *P–T–t* Paths from Individual Samples and Implications for Early Proterozoic Tectonic Evolution, *J. Petrol.*, 1991, vol. 32, pp. 139–167.

Méres, Š. and Hovorka, D., Metamorphic Development of Gneisses in the Suchý, Malá Magura and Malá Fatra Mts. (Central Slovakia), *Mineral. Slov.*, 1989, vol. 21, pp. 203–216.

Méres, Š., Ivan, P., and Hovorka, D., Garnet–Pyroxene Metabasites and Antigorite Serpentinites—Evidence of the Leptyno–Amphibolite Complex in the Branisko Mts. (Tatric Unit, Central Western Carpathians), *Mineral. Slov.*, 2000 (in press).

Messiga, B., Tribuzio, R., and Caucia, F., Amphibole Evolution in Variscan Eclogite–Amphibolites from the Savona Crystalline Massif (Western Ligurian Alps, Italy): Controls on the Decompressinal *P–T–t* Path, *Lithos*, 1992, vol. 27, pp. 215–230.

O'Brien, P.J., Partially Retrograded Eclogites of the Münchberg Massif, Germany: Records of a Multi-Stage Variscan Uplift History in the Bohemian Massif, *J. Metamorph. Geol.*, 1993, vol. 11, pp. 241–260.

O'Brien, P.J., Röhr, C., Okrusch, M., and Patzak, M., Eclogite Facies Relics and a Multistage Breakdown in Metabasites ofx the KTB Pilot Hole, NE Bavaria: Implications for the Variscan Tectonometamorphic Evolution of the Bohemian Massif, *Contrib. Mineral. Petrol.*, 1992, vol. 112, pp. 261–278.

Oberhansli, R., Candan, O., Dora, O.O., and Burr, St.H., Eclogites within the Menderes Massif, Western Turkey, *Lithos*, 1997, vol. 41, pp. 135–150.

Pattison, D.R.M. and Newton, R.C., Reversed Experimental Calibration of the Garnet–Clinopyroxene Fe–Mg Exchange Thermometer, *Contrib. Miteral. Petrol.*, 1989, vol. 101, pp. 87–103.

Peacock, S.M. and Goodge, J.W., Eclogite-Facies Metamorphism Preserved in Tectonic Blocks from a Lower Crustal Shear Zone, Central Transantarctic Mountains, Antarctica, *Lithos*, 1995, vol. 36, pp. 1–13.

Perchuk, L.L., Lavrentieva, I.V., Aranovich, L.J., and Petrík, I., Comparative Characteristics of Thermodynamic Regimes of Metamorphic Rocks from Caucasus Ridge and Western Carpathians, *Geol. Zborn.—Geol. Carpathica*, 1984, vol. 35, pp. 105–135.

Percival, J.A., High-Grade Metamorphism in the Chapleau–Foleyet Area, Ontario, *Am. Mineral.*, 1983, vol. 68, pp. 667–686.

Powell, R., Regression Diagnostics and Robust Geothermometer/Geobarometer Calibration: The Garnet–Clinopyroxene Geothermometer Revised, *J. Metamorph. Geol.*, 1985, vol. 3, pp. 327–342.

Putiš, M., Korikovsky, S.P., and Pushkarev, Yu.D., Petrotectonics of an Austroalpine Eclogite-bearing Complex (Sieggraben, Eastern Alps) and U–Pb Dating of Exhumation, *Jahrb. Geol. Bundes.*, 2000, vol. 142, pp. 73–93.

Rakús, M., Elečko, M., Gašparík, J., *et al.*, *Geological Map of the Lucánská Malá Fatra Mts. 1 : 50000*, Bratislava: D. Stur Inst. Geology, 1988.

Rubie, D.C., Role of Kinetics in the Formation and Preservation of Eclogites, Carswell, D.A., Ed., *Eclogite Facies Rocks*, Glasgow: Blackie, 1990, pp. 111–140.

Russ-Nabelek, C., Isochemical Contact Metamorphism of Mafic Schist, Laramie Anorthosite Complex, Wyoming: Amphibole Compositions and Reactions, *Am. Mineral.*, 1989, vol. 74, pp. 530–548.

Scherbak, N.P., Cambel, B., Bartnitsky, E.N., and Stepanyuk, L.M., U–Pb Age of Granitoid Rocks from the Quarry Dubná Skala–Malá Fatra Mts., *Geol. Zborn.—Geol. Carpathica*, 1990, vol. 41, pp. 407–414.

Schumacher, R., Compositions and Phase Relations of Calcic Amphiboles in Epidote- and Clinopyroxene-bearing Rocks of the Amphibolite and Lower Granulite Facies, Central Massachusetts, *Contrib. Mineral. Petrol.*, 1991, vol. 108, pp. 196–211.

Spear, F.S., *Metamorphic Phase Equilibria and Pressure–Temperature–Time Paths*, Washington: Mineral. Soc. Am. (Monograph), 1995, 2nd printing.

Spišiak, J. and Pitoňák, P., Nizke Tatry Mts. Crystalline Complex—New Facts and Interpretation (Western Carpathians, Czechoslovakia), *Geol. Zborn.—Geol. Carpathica*, 1990, vol. 41, pp. 377–392.

Spišiak, J. and Pitoňák, P., Banded Amphibolic Rocks—Pre-Variscan Basement of the Western Carpathians, *Terra Abstr., Supl. no. 2 to Terra Nova*, 1992, vol. 4, p. 63.

Stoddard, E.F., Zoned Plagioclase and the Breakdown of Hornblende in Pyroxene Amphibolites, *Can. Mineral.*, 1985, vol. 23, pp. 195–204.

Todd, C.S. and Evans, B.W., Properties of CO_2-Induced Dehydration of Amphibolite, *J. Petrol.*, 1994, vol. 35, pp. 1213–1239.